EES Catalysis

PERSPECTIVE

View Article Online
View Journal | View Issue

Check for updates

Cite this: *EES Catal.*, 2025, 3, 386

Identification of catalyst optimization trends for electrocatalytic $CO_{(2)}$ reduction to ethylene†

Stefan J. Raaijman,[a] Maarten P. Schellekens,[ac] Yoon Jun Son,[b] Marc T. M. Koper*[c] and Paul J. Corbett *[a]

In this perspective we analyze copper and copper-based electrocatalysts with high ethylene selectivities from the literature to identify global catalyst formulation trends that allow for making catalysts with improved ethylene performance for industrial application. From our analysis, we identified six trends that can aid researchers in creating novel, high selectivity electrocatalysts for the electroreduction of $CO_{(2)}$ to ethylene. These trends were as follows. (i) Tandem-type and (ii) supported-type catalysts perform relatively more poorly than other types of systems. Engineering the nanoenvironment through implementing nanoconfining morphologies (iii) or *via* the addition of polymeric additives (iv) brings about significant C_2H_4 selectivity enhancements. (v) Catalyst heterogeneity is an important driver for improving C_2H_4 selectivity. (vi) Both CO_2 and CO can serve as feedstock with little impact on maximum achievable C_2H_4 selectivity. As we identified during our study that the field lacks reproducibility of catalyst performance and independent reproduction of results, we propose several strategies on how to improve. Finally, we discuss changes that authors can implement to improve the industrial relevancy of their work.

Received 25th December 2024,
Accepted 12th March 2025

DOI: 10.1039/d4ey00287c

rsc.li/eescatalysis

Open Access Article. Published on 27 2025. Downloaded on 14-02-2026 07:37:44.
This article is licensed under a Creative Commons Attribution 3.0 Unported Licence.

Broader context

Overall, these trends act as a framework for designing catalyst systems with high C_2H_4 selectivity, increasing their industrial viability. Adopting $CO_{(2)}$RR technologies at an industrial scale would allow for minimal changes to existing industrial infrastructure and chemical processes whilst reducing the carbon footprint of the molecules and materials in use today, provided that the required $CO_{(2)}$ and (electrical) energy are procured from non-fossil sources.

1. Introduction

Electrochemical CO_2 reduction is a theoretically viable technology to produce various industrially desirable molecules. Products include chemical feedstocks such as CH_4,[1–3] C_2H_4,[4–6] C_2H_6,[7,8] C_3H_8,[9] EtOH,[10–13] PrOH[14–17] and various other oxygenates.[18–22] Importantly, it is possible to generate these products in a single electrochemical reactor, directly from CO_2 and H_2O as carbon- and proton sources, respectively. When supplying such a device with renewable power and CO_2 procured from non-fossil-based sources, one can produce green[23] commodity chemicals with a low carbon footprint. Multiple techno-economic assessments have reported on the industrial viability of carbon-based electrolysis for particular products.[24–27] These studies find that 'simple', *i.e.*, less reduced, 2-electron ($2e^-$) products have the strongest business case, typically comprising CO, HCOOH and syngas.[27] In part, this is because energy efficiency and catalyst selectivity – denoted by the faradaic efficiency (FE) in an electrochemical context – are critical in deciding whether the techno-economics are favorable.[24] Nonetheless, even though the electrochemical synthesis of these $2e^-$ products appears promising, industrialization of the technology has been slow with only few (mostly start-up) companies involved in upscaling the technology, including Twelve, CERT Systems, Toshiba, Siemens, Dioxycle, Avantium and GAFT. Overall, CO_2 reduction reaction (CO_2RR) technologies are still at a low technology readiness level (TRL), especially when considering further reduced ($\geq 4e^-$) products like C_2H_4.

Industrially, carbon–carbon coupled products appear compelling considering their prevalence in existing processes. However, electrocatalysts that generate such C_{2+} products typically perform poorly from either an energy efficiency perspective or from a selectivity perspective, making them less

[a] *Energy Transition Campus Amsterdam, Shell Global Solutions International B.V., Grasweg 31, 1031 HW Amsterdam, The Netherlands. E-mail: paul.corbett@shell.com*
[b] *Shell International Exploration and Production Inc., Houston, Texas 77079, USA*
[c] *Leiden Institute of Chemistry, Leiden University, PO Box 9502, 2300 RA Leiden, The Netherlands. E-mail: m.koper@lic.leidenuniv.nl*

† Electronic supplementary information (ESI) available. See DOI: https://doi.org/10.1039/d4ey00287c

© 2025 The Author(s). Published by the Royal Society of Chemistry

Open Access Article. Published on 27 2025. Downloaded on 14-02-2026 07:37:44.
This article is licensed under a Creative Commons Attribution 3.0 Unported Licence.

economically attractive. Furthermore, additional costs are incurred when a catalyst requires acidic CO_2 to react at an alkaline interface to yield high selectivities,[28,29] considering that bicarbonate and carbonate ions will form and potentially migrate to the anode where they are converted back into CO_2 and mix with the produced O_2 in the absence of a separator or when diaphragms or anion-exchange membranes are used as separators.[30] Although various strategies exist to mitigate the crossover of these ions, such as *e.g.*, preventing their migration *via* using cation-exchange membranes (CEMs)[31] and/or bipolar membranes (BPMs);[32,33] suppressing their concentration through using either humidified CO_2 or pure water-based/acidic electrolytes at the cathode;[34] or to circumvent their formation entirely by reacting CO instead of CO_2, each of these strategies have their own drawbacks. For example, BPM systems incur voltage penalties related to the splitting of water, CEM systems (when using non-acidic anolytes) will result in cation buildup at the cathode, acidic systems require operation at high current densities to increase the local pH so-as to increase the catalyst's C_2H_4 selectivity in addition to needing acidic anolyte in order to prevent cation buildup, and using CO as a substitute reactant results in additional costs being incurred to convert CO_2 to CO *via* an additional process such as *e.g.*, the reverse water–gas shift (rWGS) process.

Although the electrochemical production of C_{2+} products is not straightforward and (currently) significantly more costly than $2e^-$ products, C_{2+} products have the advantage that there are a wide range of mature chemical processes and infrastructure available for their transportation and interconversion on large scale. For instance, C_2H_4[35] and EtOH[36] are ubiquitous platform chemicals with large markets, where C_2H_4 is favorable over EtOH from a system perspective on account of it being easier to separate as it is a gas under typical reaction conditions. In addition, replacing conventional, complex lineups for C_2H_4 production from CO_2 with a single-step conversion would in principle allow for significant process simplification. Additionally, alcohols tend to chemically degrade the membranes that are typically used in electrochemical cells,[37,38] whereas C_2H_4 will not.

Based upon these considerations, we investigate herein the potential industrial applicability of the electrochemical production of C_2H_4 by studying existing literature on the catalyst formulation of electrochemical systems with high C_2H_4 selectivity to identify trends for improving C_2H_4 selectivity. We focus our investigation on specifically the cathode electrocatalyst as this component directly impacts the product distribution and cathodic activation losses when operating at a given rate of production. Hence, cathode performance dictates the system's selectivity and a significant proportion of the total energy losses. In addition, maximum current density, which is also largely determined by the electrocatalyst's properties, scales linearly with system size (and thus capital expenditure, CapEx) when normalized to production capacity. Furthermore, catalyst durability plays an integral role with respect to industrial viability with a minimum of 5000 h of operability having been proposed as a figure of merit for commercial deployment of carbon-based electrolysis technology.[39] Beyond a minimum threshold (5000 h only equating to *ca.* 7 months), catalyst durability also influences maintenance frequency and the rate at which consumables (*e.g.*, gas diffusion electrodes or catalyst coated membranes) must be replaced when the catalyst is the limiting component, driving up operational expenditure (OpEx). Therefore, the properties of the cathode catalyst are one of the decisive factors in determining the economic viability of an electrochemical C_2H_4 production plant. To this end, we reviewed high-performance C_2H_4 catalyst systems from the literature to determine (a) what is experimentally achievable and (b) which factors determine why certain catalyst systems exhibit superior performance.

In general, determining standardized catalyst performance for industrial application requires a comprehensive study under (i) industrial conditions in (ii) an optimized device. Namely, determining *e.g.*, maximum achievable current densities and energy efficiencies of an industrial system depends not only on the catalyst material itself but also on *e.g.*, its distribution and loading, and the reactant/product mass transport properties of the electrode. Determining lifetime similarly necessitates industrial testing conditions and an optimized system for obtaining representative results. Importantly, accurately estimating standardized catalyst performance through extrapolation of results obtained under non-industrial conditions with unoptimized systems is a difficult task to achieve. This realization is an important one, given that optimizing every single component of an electrochemical cell (or stack) and measuring performance under industrial conditions is typically beyond the scope of most scientific works, which are the source of information for this perspective. As such, values for the maximum current density, cell voltage and lifetime as reported in scientific publications are of limited use in assessing the industrial applicability of the corresponding catalyst systems.

The remaining commonly reported metric is product selectivity, which is mostly determined by intrinsic catalyst activity and less by engineering constraints. Although not without its flaws (such as the effect of feedstock conversion level on selectivity[40]), such limitations can generally be remedied *via* a thorough experimental design. Because of this, we consider product selectivity to be a valuable indicator of industrial performance, and we use it in this study to investigate catalysts' 'industrial potential'. We achieved this through compiling a list of highly selective C_2H_4 electrocatalysts, which we subsequently analyzed to identify global trends with respect to favorable catalyst properties and/or characteristics for achieving exceptional C_2H_4 selectivity. We place an emphasis on bi- and multi-elemental catalyst systems on account of their increased degrees of freedom, which is beneficial for optimization.

Overall, our study shows that 75–80% C_2H_4 can be obtained reliably under industrially relevant conditions using either CO_2 or CO as reactants. Here, we use the word 'reliably' to denote 'reported by multiple authors for different catalyst systems', rather than 'having high system stability'. Tandem-type and supported-type catalysts were found to perform relatively more poorly than other types of systems, though their activity can be improved under specific circumstances. We hypothesize that substrates with inherent C_2H_4 activity make for good supporting materials and provide ample non-copper based materials that could be used to test this. We repeatedly observe the

Open Access Article. Published on 27 2025. Downloaded on 14-02-2026 07:37:44.
This article is licensed under a Creative Commons Attribution 3.0 Unported Licence.

importance of the microenvironment, with nanoconfining morphologies and polymeric additives bringing about the largest C_2H_4 selectivity enhancement. However, we also identified that reproducibility of catalyst performance and independent reproduction of (promising) results are lacking, for which we propose several strategies for improvement. Finally, we discuss how additional industrial relevance can be achieved with relatively little extra experimental burden.

2. Data discussion

Summary tables of the high selectivity C_2H_4 electrocatalysts identified in this study, making a minimum of 40% C_2H_4 for metallic and oxide-derived Cu systems and a minimum of 25% C_2H_4 for multi-elemental systems, are provided in the ESI.† They have been grouped (categorized) primarily based on their elemental composition, with the exception of polymer-based systems which were grouped separately. We chose to categorize the catalyst systems in this way to maintain some degree of chemical comparability within each group. This has resulted in the following tables:

- Pure metallic copper catalysts, summarized in Table S1 (ESI†).
- Oxide-derived copper catalysts, summarized in Table S2 (ESI†).
- Bi-elemental Cu/M catalysts with M = Al, B, Mg, Zn, Sn, Pd, Pb, Ni, Co, Ga, Fe, Au, Ag, [Zr & Hf], Ti, Si, Lanthanides (Ce, [La, Pr, Nd, Eu, Sm & Gd]) and carbon/C are summarized in Tables S3–S22 (ESI†) whilst a final group consisting of bi-elemental catalysts with insufficient sources (≤ 3) consisting of [Pt, Sb, Bi, Sr, Se, Mo, Mn, Ru, Rh, Sc, Ge, In & W] is summarized in Table S23 (ESI†).
- Multi-elemental Cu/$\sum$M catalysts (≥ 3 metallic elements), summarized in Table S24 (ESI†).
- Polymeric core/shell-type Cu catalysts consisting of a metallic or oxide-derived copper core with either an organic or inorganic layer/shell, summarized in Table S25 (ESI†).
- Metallic or oxide-derived Cu catalysts post-modified with an organic and/or inorganic coating/overlayer, summarized in Table S26 (ESI†).

The first Section 2.1 will focus on metallic and oxide-derived copper catalysts, to define a baseline of what pure copper is capable of. However, many works have investigated if the inherent selectivity of copper can be improved through the addition of various other components ('copper-based' systems). Many such copper-based systems can be categorized as bi-elemental systems, denoted herein as Cu/M (*e.g.*, Cu + co-element M). Bi-elemental systems with M = Al, B, Mg, Zn, Sn, Pd, Pb, Ni, Co, Ga, Fe, Au, Ag, [Zr & Hf], Ti, Si, Lanthanides (Ce, [La, Pr, Nd, Eu, Sm & Gd]) and carbon/C have been summarized in Tables S3–S22 (ESI†), whilst bi-elemental systems having ≤ 3 sources have been grouped together in a miscellaneous category, comprising [Pt, Sb, Bi, Sr, Se, Mo, Mn, Ru, Rh, Sc, Ge, In & W] and are summarized in Table S23 (ESI†). Considering that the bi-elemental systems were found to be less common than metallic and oxide-derived copper systems, we opted to decrease our selection criteria to systems making $\geq 25\%$ C_2H_4 instead of $\geq 40\%$ C_2H_4 to increase the likelihood of achieving statistically relevant numbers of sources on a per-element basis for our analysis. A small number of publications even report on multi-elemental systems (total metallic elements of ≥ 3) with $\geq 25\%$ C_2H_4 selectivity, denoted herein as Cu/$\sum$M, as summarized in Table S24 (ESI†). Finally, we identified two additional categories for systems that are differentiated by the presence of an organic and/or inorganic component – either in the form of a polymeric core/shell-type morphology (comprising a metallic or oxide-derived copper core and an organic or inorganic shell, Table S25, ESI†) or metallic or oxide-derived Cu catalysts that have been post-modified with an organic and/or inorganic overlayer, summarized in Table S26 (ESI†).

Compared to metallic and oxide-derived copper, the copper-based systems are significantly more heterogeneous, *e.g.*, having more (initial) chemical states accessible, with many interfaces existing between chemically distinct particles and individual atoms, having large differences in electrical and thermal conductivities, having large variations in surface hydrophobicity, *etc.* Importantly, even with our reduced selection criterium of $\geq 25\%$ C_2H_4, the number of publications reporting on bi- and multi-elemental catalysts of a given composition that meet this criterium typically does not exceed 10. As such, we analyze the entirety of the dataset (including metallic and oxide-derived Cu) from a holistic perspective rather than on a per-elemental basis to identify global trends regarding what makes for a highly selective C_2H_4 electrocatalyst from Section 2.2 and beyond. With this we mean to say that we look at the overall dataset for trends that are shared across systems rather than elemental composition-specific trends, which we will interchangeably refer to as holistic or global observations/trends.

Although we will look at the dataset from a holistic perspective on account of the small sample size on a per-element basis, brief descriptions of all the tabulated systems have been provided in the ESI.† We opt for not including this information in the main text to allow us to focus on the main goal of this study: to identify and discuss global trends with respect to favorable catalyst properties and/or characteristics for achieving high C_2H_4 selectivity from electrochemical $CO_{(2)}$ reduction on copper-based catalysts. However, it is the dataset on a whole that gives us the confidence to make the claims we do herein, which is why all investigated systems are included in the ESI† as opposed to only those systems that are directly relevant. Importantly, alkaline CO_2 systems are omitted from our analyses (unless stated otherwise) on account of the unsustainable costs associated with maintaining a local alkaline pH in the presence of CO_2 which necessitates continual HCO_3^-/CO_3^{2-} removal.[30] Further details regarding how catalysts were identified and selected are provided in the ESI.† A high-level overview of the catalyst systems studied in this work is provided in Fig. 1, depicting the spread of the C_2H_4 FEs for various catalyst systems with differing elemental compositions together with the number of identified publications for the various categories.

2.1. Feedstock agnosticism

For the purposes of this manuscript, metallic copper-based electrocatalysts are used as a reference point of what level of

© 2025 The Author(s). Published by the Royal Society of Chemistry

Open Access Article. Published on 27 2025. Downloaded on 14-02-2026 07:37:44.
This article is licensed under a Creative Commons Attribution 3.0 Unported Licence.

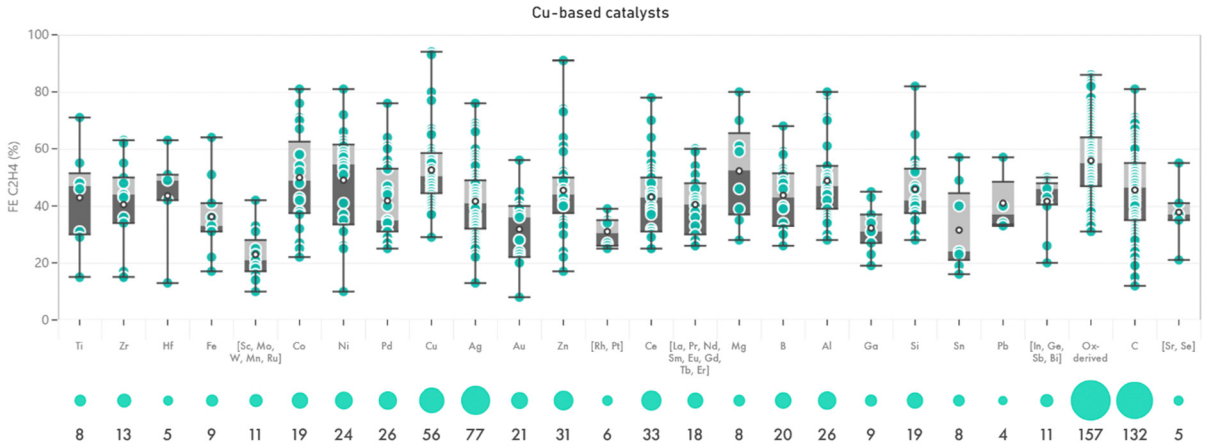

Fig. 1 High-level overview of the catalyst systems compiled in this work, depicting the maximum C_2H_4 FE distribution for the catalyst systems as grouped based on their elemental composition, together with the number of sources identified for each of these categories.

performance is achievable in the absence of convoluting effects, with a summary of their selectivities and characteristics being presented in Table S1 (ESI†). We consider the dataset sufficiently large to omit alkaline CO_2RR systems (15 out of 56 entries) from our analysis. Overall, we reliably observe maximum C_2H_4 FEs between 50–60%, with outliers yielding 77%[41] and 93%.[42] Notably, for systems that yield $\geq$55% C_2H_4, the feedstock distribution is relatively equal with 6 entries using CO_2 as a reactant and 4 entries using CO (*i.e.*, a CO_2 : CO ratio of 1.5×). In addition, many of these systems (7 out of 10 entries) were operated at $>|-100|$ mA cm^{-2}. However, we observe that the majority of the metallic Cu systems consist of the same catalyst, namely sputter-deposited copper. As such, the number of unique metallic Cu catalyst systems is considerably less than the number of entries in the table implies, because each publication is added as a new entry even when the reported catalyst is equal to a different publication.

As a variation on- and follow-up to metallic copper, we compiled in Table S2 (ESI†) the performance of oxide-derived copper. Oxide-derived was interpreted freely to mean any catalyst with the generic formula CuX, where X constitutes either (i) a highly electronegative element or (ii) an alkali metal. In practice, this translates to X = Li, Na, K, Rb, Cs, N, O, P, S, F, Cl, Br and/or I, and combinations thereof. In alignment with the metallic copper dataset, the oxide-derived dataset was sufficiently large to allow us to omit alkaline CO_2RR systems (60 out of 157 entries) from our analysis. We find that the maximum C_2H_4 FEs reported for oxide-derived Cu catalysts outperform metallic Cu catalysts by *ca.* 10%, with C_2H_4 FEs reliably observed between 60–70% (*vs.* 50–60% for metallic Cu) and outliers yielding 76–85%.[5,43–45] For systems that yield $\geq$55% C_2H_4, we find a relatively asymmetrical feedstock distribution with 38 entries using CO_2 and 8 entries using CO as a reactant (*i.e.*, a CO_2 : CO ratio of 4.75). Furthermore, it can be observed that relatively few systems (14 out of 46 entries) were operated at $>|-100|$ mA cm^{-2}. Considering the *ca.* 10% outperformance in maximum C_2H_4 FEs of oxide-derived Cu *vs.* metallic Cu, it is also interesting to look at the $\geq$65% C_2H_4 range as a comparison. By doing so, we find that the feedstock imbalance (CO_2 : CO ratio) for oxide-derived systems is significantly reduced, dropping from 4.75 to 2.3 (*vs.* 1.5 for metallic Cu) whilst high-current density systems become somewhat more common, increasing from 14 out of 46 entries to 9 out of 23 entries (*vs.* 7 out of 10 entries for metallic Cu).

Metallic and oxide-derived Cu systems exhibit similarities as well. For instance, both CO_2 and CO can serve as the feedstock for high selectivity ($\geq$55% C_2H_4) systems. Additionally, top-tier catalysts (on a selectivity basis) also exhibit similar performance, yielding 77–93%[41,42] for metallic Cu systems *vs.* 76–85%[5,43–45] for oxide-derived Cu systems. The main difference seems to be that oxide-derived Cu catalysts yield maximum C_2H_4 FEs that are *ca.* 10% higher than metallic Cu catalysts when looking at the $\geq$55% range. We hypothesize this performance gap it is not unreasonable when considering the propensity of oxide-derived copper to reconstruct into smaller (higher active area) particles which are rich in undercoordinated sites.[46] Although not necessarily more active, Kim *et al.* show that such sites can act as CO reservoirs, resulting in higher overall turnover frequencies (TOFs) towards C_2H_4 of the 'real' catalytically active sites.[47]

This overview of metallic and oxide-derived Cu systems serves as a benchmark of what can be reasonably expected of primarily copper-based electrocatalysts in terms of C_2H_4 performance. It also yields our first global observation, namely that both CO_2 and CO can be used as feedstock for high selectivity C_2H_4 electrocatalysts with little difference in maximum achievable performance provided that the alkaline CO_2RR effect is accounted for (achieved herein through omitting such systems from the analysis). Although the current discussion focused on metallic and oxide-derived copper systems, the feedstock agnosticism is found to be present also when we consider the entirety of the dataset. This can be seen from Table 1, wherein catalyst systems with the highest C_2H_4 selectivities as identified in the current work ($\geq$70% C_2H_4) are summarized. Although this table is discussed in further detail in Section 2.6, it can be observed that both CO_2 and CO are present as feedstocks for these top-performing systems, including for various copper-based systems.[44,48,49]

© 2025 The Author(s). Published by the Royal Society of Chemistry

Open Access Article. Published on 27 2025. Downloaded on 14-02-2026 07:37:44.
This article is licensed under a Creative Commons Attribution 3.0 Unported Licence.

Table 1 List of top-performing C_2H_4 electrocatalysts (≥70% FE max for C_2H_4). Alkaline CO_2RR systems are shaded red whilst CORR systems are shaded blue

#	Electromaterial description	Catalyst type	Majority elements	Polymeric / (in-) organic additives	Catholyte	Membrane	Reactant	E	j	Max.C_2H_4 FE	Ref.
1	50 μm Cu-exchanged stannosilicate UZAR-S3 'mixed matrix membrane' toplayer, on a PVA/Chitosan midlayer, on a commercial 70 nm Cu NPs with chitosan bio-based polymeric binder underlayer, on Toray TGP-H-60 GDL (exact conditions ambiguously reported)	Overlayer	Cu	Chitosan, Cu exchanged stannosilicate UZAR-S3, polyvinylalcohol	-	Sustainion X-37 50 grade	CO_2	-0.87 V vs. RHE	-10 mA/cm^2	98	196
2	Commercial 70 nm Cu NPs with chitosan bio-based polymeric binder, on Toray TGP-H-60 GDL	Metallic Cu	Cu	Chitosan	-	Sustainion X-37 50 grade	CO_2	-0.53 V vs. RHE	-10 mA/cm^2	94	196
3	Commercial Cu NPs (25 nm), on a GDL with custom MPL, hotpressed onto a Nafion membrane	Metallic Cu	Cu	Nafion	-	Nafion 117	CO_2	-1.7 V vs. Ag/AgCl	-7.5 mA/cm^2	93	42
4	CuO_x supported on ZnO, on carbon paper (TGP-H-60)	Mixed-phase/Janus, A-supports-B	Cu, Zn, O	Nafion	-	Nafion 117	CO_2	-2.5 V vs. Ag/AgCl	-7.5 mA/cm^2	91	127
5	Nafion overlayer covering a catalyst layer comprised of electroplated Cu modified via grafting an aryl diazonium-based polymeric coating, on GDL	Overlayer	Cu, O	Nafion, Aryl diazonium-based polymer	-	Sustainion X37-50	CO_2	-3.85 V vs. ANODE	-602 mA/cm^2	89	195
6	Poly-N-(6-aminohexyl)acrylamide-coated electrodeposited Cu dendrites on GDL	Overlayer	Cu	Poly-N-(6-aminohexyl)acrylamide	10 M KOH	?	CO_2	-0.47 V -iR vs. RHE	?	87	4
7	Template-assisted electroplated nanoporous (20 nm pore diameter) CuO_x overlayer on Cu foam	Oxide-derived	Cu, O	-	-	X37-50 Grade 60	CO_2	-3.0 V vs. ANODE	-368 mA/cm^2	86	197
8	Electroplated Cu modified via grafting an aryl diazonium-based polymeric coating (without Nafion toplayer), on GDL	Core/shell (in-)organic	Cu, O	Aryl diazonium-based polymer	-	Sustainion X37-50	CO	-2.5 V vs. ANODE	-179 mA/cm^2	86	195
9	Amorphous CuO_x film evaporation-deposited on GDL	Oxide-derived	Cu, O	-	0.5 M $KHCO_3$	"Nafion"	CO_2	-1.3 V - iR vs. RHE	-32 mA/cm^2	85	45
10	KOH anodization-derived CuO nanoplate on Cu-sputtered GDL	Oxide-derived	Cu, O	-	-	Sustainion X37-50	CO_2	-0.81 V - iR vs. RHE	-100 mA/cm^2	84	6
11	TiO_2 NPs supported on V/Cu-based layered double hydroxide, on carbon paper	Mixed-phase/Janus, A-supports-B	Cu, V, Ti, O	Nafion	0.1 M $KHCO_3$	Nafion 117	CO_2	-0.4 V vs. RHE	-7 mA/cm^2	84	198
12	Defective CuO-derived Cu nanosheets, on glassy carbon	Oxide-derived	Cu, O	Nafion	0.1 M K_2SO_4	Nafion 117	CO_2	-1.18 V - iR vs. RHE	-60 mA/cm^2	83	5
13	Pre-reduced, CuO-derived Cu quantum dots (5 nm), on a GDL	Oxide-derived	Cu, O	-	1.0 M KOH	FAA-3-PK-75	CO_2	-0.93 V -iR vs. RHE	-1100 mA/cm^2	82	199
14	$CuSiO_3$ coated on ordered porous CuO prepared from mesoporous SiO2 molecular sieve starting material, supported on carbon, on "GDE"	Core/shell, atomically mixed/crystalline	Cu, Si, O, C	Nafion	1.0 M KOH	FAA-PK-130	CO_2	-1.18 V vs. RHE	-400 mA/cm^2	82	132
15	Ultrathin (ca. 4.8 nm) alloyed hexagonal CuNi nanosheets (ca. 1:1 atom ratio), on Ti mesh	Alloyed/Doped	Cu, Ni	Nafion	0.5 M $KHCO_3$	?	CO_2	-1.5 V vs. RHE	-470 mA/cm^2	81	128
16	Ultrathin (ca. 46.3 nm) alloyed hexagonal CuCo nanosheets (ca. 1:1 atom ratio), on glassy carbon	Alloyed/Doped	Cu, Co	Nafion	0.5 M $KHCO_3$	Nafion 117	CO_2	-1.5 V vs. RHE	-400 mA/cm^2	81	129
17	Cu NPs supported on Cu/SAC-graphitic carbon nitride (g-C_3N_4), on carbon paper	SAC, supported	Cu, C	-	0.1 M $KHCO_3$	Fumasep FAA-3-PK-130	CO_2	-1.28 V vs. RHE	-45[a] mA/cm^2	81	54
18	60 nm step site-rich Cu NPs blow-dried with Ar, on GDL	Metallic Cu	Cu	Sustainion XA-9	1.0 M KOH	Fumasep FAA-3-PK-75	CO_2	-0.58 V - iR vs. RHE	-710 mA/cm^2	80	33
19	CNP and graphite layer on top of chemically etched co-sputtered Cu/Al layer on PTFE GDL	Overlayer, Alloyed/Doped	Cu, Al, C	Nafion	1.0 M KOH	FAA-3-PK-130	CO_2	-1.67 V - iR vs. RHE	-400 mA/cm^2	80	200
20	Mg surface-doped CuO_x NPs ($Mg_{0.72}Cu$), on GDL	Alloyed/Doped	Cu, Mg, O	Nafion	1.0 M KOH	NEOSEPTA, AHA	CO	?	?	80	48
21	CuO NPs coated with 1-dodecanethiol, on GDL	Core/shell (in-)organic	Cu, O	Nafion, 1-dodecanethiol	1.0 M KOH	?	CO_2	-1.2 V vs. RHE	-304 mA/cm^2	80	201
22	CuO NPs supported on Al_2CuO_4 nanosheets, on glassy carbon	Mixed-phase/Janus, atomically mixed/crystalline, A-supports-B	Cu, Al, O	Nafion	0.1 M $KHCO_3$	Selemion AMV	CO_2	-0.99 V - iR vs. RHE	-2 mA/cm^2	79[a]	69
23	Calcined (in Al foil!) electroplated Cu dendrites, on GDL	Oxide-derived	Cu, O, Al (?)	Nafion	3.0 M KOH	Sustainion X37-50 Grade T	CO	?	-100 mA/cm^2	78	44
24	Amorphous CuO_x film evaporation-deposited on GDL	Oxide-derived	Cu, O	-	-	FBAPK-13	CO_2	-1.75 V vs. ANODE	-113 mA/cm^2	78	45
25	Hollow Cu/CeO_2 nanotubes composed of aggregated nanoparticles, on carbon paper - prepared by decorating electrospun polyacrylonitrile (PAN) fibres with metal and burning away the PAN	Mixed-phase/Janus	Cu, Ce, O	Nafion	1 M KOH	FAA-3-PK-130	CO_2	-0.7 V vs. RHE	-110 mA/cm^2	78	133
26	CO_2RR pre-activated defective Cu NWs, on glassy carbon (tested in semi-pulsed electrolysis mode)	Metallic Cu	Cu	Nafion	0.1 M $KHCO_3$	Nafion	CO_2	-1.01 V - iR vs. RHE	-22 mA/cm^2	77	41
27	Ag/Au (3:1 ratio) alloy, highly defective, cubic wireframe NPs (59 nm) post-modified with epitaxially deposited Cu 'overlayer', on GDL	A-supports-B, alloyed/doped	Ag, Au, Cu	-	1.0 M KOH	Fumasep FAB-PK-130	CO_2	-0.65 V - iR vs. RHE	- 305 mA/cm^2	77	134
28	Ionic liquid-coated Cu-MOF (Cu_3(1,3,5-Benzenetricarboxylic acid)$_2$), on glassy carbon	Core/shell (in-)organic	Cu	Nafion, 1,3,5-Benzenetricarboxylic acid (BTC), 1-Butyl-3-methylimidazolium nitrate (BmimNO$_3$)	0.1 M $KHCO_3$	Nafion 117	CO_2	-1.49 V vs. RHE	-34 mA/cm^2	77	202
29	Porous Cu_2O microparticles, on PTFE-modified GDL	Oxide-derived	Cu, O	Nafion	1.0 M KCl + x M H_2SO_4 (pH 1.9)	Nafion 115	CO	?	-800 mA/cm^2	76	43
30	Dilute Cu/Pd alloy (1.4 at. % Pd) prepared via co-electrodeposition, on glassy carbon	Alloyed/Doped	Cu, Pd	-	0.1 M $KHCO_3$	FAA-3-PK-75	CO_2	-0.7 V vs. RHE	-3 mA/cm^2	76	203
31	Co-TMC (tetraphenylporphyrin) confined within the nanopores of porous Cu_2O microparticles, on PTFE-modified GDL	A-supports-B, Mixed-phase/Janus	Cu, O, Co	Nafion	1.0 M KCl + x M H_2SO_4 (pH 1.9)	Nafion 115	CO	?	-800 mA/cm^2	76	43
32	Ag foil coated with Cu NP Nafion ink	Overlayer	Cu, Ag	Nafion	0.1 M $NaHCO_3$	-	CO_2	-1.9 V vs. RHE	-21 mA/cm^2	76	147
33	Prepared by electrodepositing Cu on Ag surfaces	Overlayer	Cu, Ag	Nafion	0.1 M $NaHCO_3$	-	CO_2	-1.9 V vs. RHE	-21 mA/cm^2	76	148
34	Defect-rich CuO NRs (800 nm) with HCOO- induced pores, on a GDL	Oxide-derived	Cu, O	Nafion	2.0 M KOH	Nafion 117	CO_2	-0.8 V -iR vs. RHE	-144 mA/cm^2	75	204

© 2025 The Author(s). Published by the Royal Society of Chemistry

Open Access Article. Published on 27 2025. Downloaded on 14-02-2026 07:37:44.
This article is licensed under a Creative Commons Attribution 3.0 Unported Licence.

Table 1 (*continued*)

35	Star shaped (322)-rich Cu_2O large NPs, on glassy carbon	Oxide-derived	Cu, O	Nafion D-521	0.1 M $KHCO_3$	Nafion	CO_2	-1.2 V vs. RHE	-11 mA/cm^2	74	205
36	Brass foil (62% Cu, 37% Zn, trace amounts of Fe, Pb, Sn) with Nafion/PVDF (70:30 wt%) overlayer	Alloyed/Doped, Overlayer	Cu, Zn	Nafion, PVDF	0.1 M $NaHCO_3$	-	CO_2	-0.89 V vs. RHE	?	74	149
37	N-doped CuO_x NPs derived from calcination of $Cu(OH)_3NO_3$ precursor at 350 °C, on GDL	Oxide-derived	Cu, O, N	Nafion	1 M KOH	Fumasep-FAA-3-PK-130	CO_2	-1.09 V - iR vs. RHE	-962[c] mA/cm^2	73	206
38	Highly porous Zn/Cu layer (10 at. % Zn) generated through partially leaching of co-sputtered Zn/Cu layer on PTFE substrate	Alloyed/Doped	Cu, Zn	-	0.75 M KOH	Fumasep FAB-PK-130	CO_2	-1.1 V vs. RHE	-150 mA/cm^2	73	176
39	N1-/N3-substituted imidazolium-based overlayer on Cu plate	Overlayer	Cu	N1-substituted (1,10-phenanthrolinyl) and N3-substituted (n-butyl) imidazolium	0.1 M $KHCO_3$ (pH 6.8)	"Hangzhou Huamo Technology Co., Ltd"	CO_2	-1.24 V vs. RHE	-6 mA/cm^2	73	207
40	(220)-facet rich CuI nanodots (5.3 nm) prepared via in-situ reduction of $Cu(OH)_2$) NPs on carbon paper GDL in 0.1 M $KHCO_3$ + 0.1 M KI	Oxide-derived	Cu, O, I	Nafion	0.5 M $KHCO_3$ + 0.5 M KI	FAA-3-PK -130	CO_2	-2.1 V vs. RHE	-800 mA/cm^2	72	208
41	Cu NPs encapsulated in mesoporous Ni-SAC functionalized carbon, on GDL	Mixed-phase/Janus, A-supports-B	Cu, Ni, C, N	-	1.0 M $KHCO_3$	"Fuel Cell Store"	CO_2	-1.1 V -iR vs. RHE	-406 mA/cm^2	72	130
42	Ag-doped $La_{2-x}Ag_xCuO_{4-\delta}$ NPs (x=0.2) with oxygen vacancies, on Toray carbon paper	Atomically mixed/Crystalline, alloyed/doped	Cu, Ag, La	Nafion	0.5 M $KHCO_3$	Nafion	CO_2	-1.1 V vs. RHE	-28 mA/cm^2	72	209
43	CuO_x NPs (large size distribution) mixed with PTFE, on carbon paper	Core/shell (in-)organic	Cu, O	Nafion, PTFE	0.5 M KCl + 50 mM benzyl alcohol	FKB PK 130	CO_2	-1.38 V vs. RHE	-88 mA/cm^2	72	210
44	N-arylpyridinium electrodeposition-modified Cu-sputtered PTFE GDL	Overlayer	Cu	N,N′-(1,4-phenylene) bispyridinium salt	1.0 M $KHCO_3$	Fumapem FAA-3-PK-130	CO_2	-0.83 V -iR vs. RHE	-325 mA/cm^2	72	211
45	Poly-N-(6-aminohexyl)acrylamide-coated electrodeposited Cu dendrites on GDL	Overlayer	Cu	Poly-N-(6-aminohexyl)acrylamide	1.0 M KOH	?	CO_2	-0.97 V -iR vs. RHE	-433 mA/cm^2	72	4
46	Grainboundary-rich $Cu_2CO_3(OH)_2$-derived Cu nanoribbons with Carbon NP midlayer and graphite toplayer, on PTFE GDL	Oxide-derived	Cu, O, C	-	1.0 M KOH	Fumapem FAA-3-PK-130	CO_2	-1.6 V vs. RHE	-700 mA/cm^2	71	212
47	Cu_2O NCs on GDL, electrochemically pre-activated via in-situ reduction in the presence of CO_2	Oxide-derived	Cu, O	Nafion	1.0 M KOH	Sustainion® X37-50 grade RT	CO_2	-0.6 V vs. RHE	-207 mA/cm^2	71	213
48	Defect-rich CuO NRs (800 nm) with HCOO- induced pores, on a GDL	Oxide-derived	Cu, O	Nafion	3.0 M KCl	Nafion 117	CO_2	-1.07 V -iR vs. RHE	-312 mA/cm^2	71	204
49	CuO_x nanocubes/rectangles supported on Al_2O_3 nanosheets having an Al_2CuO_2 interface layer, mixed with CNPs, on glassy carbon	Mixed-phase/Janus, atomically mixed/crystalline, A-supports-B	Cu, Al, O, C	Nafion	0.1 M $KHCO_3$	Nafion 117	CO_2	-1.2 V - iR vs. RHE	-60 mA/cm^2	71	70
50	Cu_2O NCs supported on cobalt phthalocyanine-modified-acetylene black, on GDL	A-supports-B, Mixed-phase/Janus	Cu, Co, C	Nafion	1.0 M KOH	FAA-3-20	CO_2	-0.76 V - iR vs. RHE	-317 mA/cm^2	71	214
51	Single atom Cu supported on ultrathin $Ti_3C_2T_x$ nanosheets, on carbon paper	Single atom	Cu, C, Ti	Nafion	1.0 M KOH	Nafion 117	CO	-0.70 V vs. RHE	-23 mA/cm^2	71	49
52	Cu_2O NPs supported on CNTs modified with Cu-based COF, on glassy carbon	COF, supported	Cu, C, O	Nafion	0.5 M $KHCO_3$	Nafion 117	CO_2	-1.1 V vs. RHE	-44 mA/cm^2	71	215
53	Thin quasi-graphitic carbon-shell functionalized, N-doped Cu NPs supported on carbon fibers, on GDL	Core/shell	Cu, C, N	Nafion, quasi-graphitic carbon shell	1.0 M KOH	Sustanion X37-50	CO_2	-0.69 V -iR vs. RHE	-400 mA/cm^2	71	216
54	Single atom Cu sites enclosed in an Ir-containing Zr-based MOF framework with rod-like morphology, on carbon cloth	Single atom, Atomically mixed/Crystalline	Cu, Ir, Zr	Nafion	1.0 M phosphate buffer saline	Nafion 212	CO_2	-1.0 V vs. RHE	-28 mA/cm^2	71	131
55	Sputtered Cu with Carbon NP midlayer and graphite toplayer, on PTFE GDL	Oxide-derived	Cu, C	-	7.0 M KOH	Fumasep FAB-PK-130	CO_2	-0.57 V - iR vs. RHE	-100 mA/cm^2	70	217
56	$Cu_3(PO_4)_2$ particles, on glassy carbon	Oxide-derived	Cu, O, P	Nafion	0.1 M $KHCO_3$	Nafion 117	CO_2	-1.45 V vs. RHE	-23 mA/cm^2	70	218
57	Iodine-doped copper oxychloride NPs, on glassy carbon	Oxide-derived	Cu, O, Cl, I	Nafion	0.05 M $KHCO_3$	-	CO_2	-1.71 V vs. RHE	-29 mA/cm^2	70	219
58	Wet-chemical induced ($NaOH$ / $(NH_4)_2S_2O_8$) high roughness nanoporous CuO_x layer on Cu plate	Oxide-derived	Cu, O	-	1.0 M KOH	"Nafion"	CO	-0.8 V vs. RHE	-130 mA/cm^2	70	220
59	Template-assisted electroplated nanoporous (20 nm pore diameter) CuO_x overlayer on Cu plate	Oxide-derived	Cu, O	-	0.1 M $KHCO_3$	Nafion 117	CO_2	-0.99 V vs. RHE	-63 mA/cm^2	70	197
60	CuO NPs supported on Al_2CuO_4 nanosheets, on GDL	Mixed-phase/Janus, atomically mixed/crystalline, A-supports-B	Cu, Al, O	Nafion	1.0 M KOH	FAA-3-PK-130	CO_2	-2.03 V - iR vs. RHE	-600 mA/cm^2	70	69
61	Mg surface-doped CuO_x NPs ($Mg_{0.72}Cu$), on GDL	Alloyed/Doped	Cu, Mg, O	Nafion	1.0 M KOH	NEOSEPTA, AHA	CO_2	-0.69 V - iR vs. RHE	-650 mA/cm^2	70	48
62	Cold H_2 plasma-treated porous mixed CoO_x/CuO_x, on glassy carbon	Mixed-phase/Janus	Cu, Co	Nafion	0.1 M $KHCO_3$	?	CO_2	-1.0 V vs. RHE	-21 mA/cm^2	70	221
63	Hollow Cu/CeO_2 nanotubes composed of aggregated nanoparticles, on carbon paper - prepared by decorating electrospun polyacrylonitrile (PAN) fibres with metal and burning away the PAN	Mixed-phase/Janus	Cu, Ce, O	Nafion	0.1 M K_2SO_4	Nafion 117	CO_2	-1.1 V vs. RHE	-25 mA/cm^2	70	133
64	Cu_3(2,3,6,7,10,11-hexaiminotriphenylene)$_2$ MOF supported on Ketjen Black, on glassy carbon	MOF, supported	Cu, O, C	Nafion	0.1 M $KHCO_3$	Nafion	CO_2	-1.37 V - iR vs. RHE	-38 mA/cm^2	70	50
65	In-situ formed Cu_2O ultra-small NPs derived from CO_2RR/KCl electro-activated Cu(Pyrazole)2 MOF, on carbon paper	MOF, supported	Cu, O, C, N	Nafion	0.1 M KCl	Nafion	CO_2	-1.03 V - iR vs. RHE	-18 mA/cm^2	70	51
66	Sputtered Cu with Carbon NP midlayer and graphite toplayer, on PTFE GDL	Overlayer	Cu, C	CNPs, Graphite	7.0 M KOH	Fumasep FAB-PK-130	CO_2	-0.57 V - iR vs. RHE	-100 mA/cm^2	70	28
67	Electroplated Cu (60 s @ 400 mA/cm^2) from $CuBr_2$/tartrate/1 M KOH-containing bath with active CO_2 flow (though CO also seems to work), with Carbon NP midlayer and graphite toplayer, on Cu-sputtered PTFE GDL (ambiguously reported)	Overlayer	Cu, C	CNPs/Nafion, Graphite/Nafion	7.0 M KOH	Fumapem FAA-3-PK-130	CO_2	-0.67 V - iR vs. RHE	-280 mA/cm^2	70	222
68	Carbon black NP (XC72R) overlayer on top of Cu-sputtered PTFE GDL	Overlayer	Cu, C	Nafion	0.5 M $KHCO_3$ + 0.5 M KCl	Nafion 117	CO_2	-0.89 V -iR vs. RHE	-500 mA/cm^2	70	223

[a] ESI erroneously reports partial $j_{C_2H_4}$@80.73% C_2H_4 as 60.15 mA cm^{-2}, report here image-extracted j_{total}. [b] Main text states 79.4%, ESI states 82.4%. Report here main text value. [c] Derived from $FE_{C_2H_4}$ and $j_{C_2H_4}$ as opposed to the reported LSV.

Open Access Article. Published on 27 2025. Downloaded on 14-02-2026 07:37:44.
This article is licensed under a Creative Commons Attribution 3.0 Unported Licence.

2.2. Support effect

In this section, we investigate a series of observations we colloquially refer to as the 'support effect', pertaining to systems wherein the active catalyst is supported on (or physically mixed with) nm μm^{-1}-sized secondary particles with a different chemical composition than the primary (C_2H_4-forming) catalyst. We have identified several trends regarding such supported-type catalysts that occur repeatedly across a variety of different systems, allowing us to garner insights for improving C_2H_4 selectivity. The majority of supported-type systems identified in this work consist of carbon-supported catalyst systems, which are included in Table S22 (ESI†) as part of the Cu/C summary. We find that these carbon-supported catalytic systems exhibit relatively poor C_2H_4 selectivity overall (*i.e.*, $\leq$60% C_2H_4), though outliers yielding between 60–70%[50–53] and even up to 81%[54] C_2H_4 exist. Importantly, Cu supported on commercially available, pristine carbon nanoparticles (CNPs, *e.g.*, Ketjen Black[46] and Vulcan XC-72[55]) reliably yield $\leq$55% C_2H_4. Increased C_2H_4 selectivity is primarily observed for systems containing chemically modified carbon supports as prepared *via e.g.*, hetero atom-functionalization,[54,56,57] organic functionalization with hetero atom-containing ligands,[58] or by *in situ* decomposition of copper-based complexes[50–53] such as metal–organic frameworks (MOFs), covalent organic frameworks (COFs) or transition metal complexes (TMCs). The general poor C_2H_4 selectivity of supported-type systems is not limited to (unmodified) carbon-based support materials either, with copper catalysts supported on oxidic secondary particles such as *e.g.*, ZrO_x,[59] ZnO_x,[60] TiO_x,[61] SiO_x[62–64] and CeO_x[65–67] similarly yielding 50–60% C_2H_4 at best. Importantly, the industrial viability of oxidic supports is debatable, considering such materials could potentially dissolve *in situ*, as reported for *e.g.*, SiO_x.[64,68] A notable exception to the poor overall selectivity of (oxide-) supported copper systems exists in the form of Cu supported on AlO_x-based secondary particles, with several such systems having been reported to exhibit high C_2H_4 selectivity ($\geq$70% C_2H_4) even under non-alkaline CO_2RR conditions.[69,70]

Likely, the poor selectivity of supported-type catalyst systems (*i.e.*, $\leq$60% C_2H_4) can be attributed to electrochemical competition between the supporting particles and the primary (C_2H_4-forming) catalyst through the support's inherent (parasitic) electrocatalytic activity. Namely, most particles used as support materials favor $2e^-$ products (*e.g.*, H_2, CO, HCOOH). Crucially, we have identified that supported-type copper systems can outperform unsupported copper systems when 'ideal' support materials are used. Ideal in this context refers to supports that are (i) stable *in situ*, (ii) electrochemically inert and (iii) electrically conductive. This has been demonstrated by Yeo *et al.*,[71] who used exfoliated Mg/Al-based layered double hydroxide (LDH) nanosheets to support commercial Cu nanoparticles (NPs). In their study, they observe similar CORR activity for unsupported *vs.* supported Cu NPs under 'standard' conditions, whilst addition of the supporting material allowed for increased catalyst loadings and operation at increased current densities without negatively impacting C_2H_4 selectivity. In fact, operation at elevated current densities improved C_2H_4 selectivity and was possible because it concerned a supported-type catalyst.

Lastly, we observe that it is beneficial to employ a support material which itself has some ($\leq$5% C_2H_4) intrinsic activity for C_2H_4 formation. For example, Haihong *et al.*[72] show that Cu single atom catalyst (SAC) sites supported on two-dimensional (2D) $Ti_3C_2T_x$ MXene nanosheets (T_x denoting surface functional groups) can yield up to 71% C_2H_4 for the CORR. Importantly, the bare substrate sans Cu sites also exhibits C_2H_4 activity. Furthermore, the support plays an active role in the catalytic process considering that the supported Cu NPs they also test in their study perform considerably poorer than the Cu-SAC sites deposited on the same secondary particles, whilst normally SACs preferentially generate C_1 products rather than carbon-coupled products.[73,74] Although supported copper systems with non-copper substrates that have inherent C_2H_4 activity are rare, we managed to identify four additional publications reporting on such systems, namely Cu supported on: Ti nanotubes[61] (55% C_2H_4), Mg/Al LDHs[71] (46% C_2H_4), carbon-based quantum dots[75] (46% C_2H_4) and Cu supported on a $[Ni_8(BDP)_6]$ MOF[76] (53% C_2H_4). From the limited data available, we hypothesize that (non-Cu) substrates with inherent C_2H_4 activity might be key in designing novel, high selectivity C_2H_4 supported electrocatalysts. To this end, we have identified various non-copper based materials having intrinsic capacity for making (small amounts of) C_2H_4 that could be investigated as catalyst supports, including Ti-,[49,61] Pt-,[77,78] Ag,[79,80] Ni,[81–87] Au-, Cd-,[88,89] Ru-,[90] Zn-,[91] Ce-,[92] Pd- and Sn-based[93] materials and/or intermetallics thereof,[71,85,94–105] various TMCs,[106,107] COFs,[88,89] MOFs[76,108] and enzymes,[109–111] and finally a number of metal-free[75,112–116] and metal-doped[117–120] types of carbons.

We conclude that supported-type catalyst systems have the potential to yield improved C_2H_4 selectivity under highly specific conditions as described in this section. However, the balance between the support and the copper catalyst is fragile and creating a supported system that outperforms conventional, unsupported (arguably 'self-supported') copper-based catalyst systems is an exacting task, with relatively few supported-type systems achieving high C_2H_4 selectivity.

2.3. Morphological benefits

The next global observation is regarding the beneficial effect of having a 2D nanosheet structure with respect to improving C_2H_4 selectivity. The importance of the nanosheet morphology was already partially evident when we discussed the support effect, where we noted the superior performance of Cu NP supported on 2D Mg/Al-based LDH nanosheets and Cu-SAC sites supported on $Ti_3C_2T_x$ nanosheets, with both substrates also exhibiting intrinsic C_2H_4 activity. However, more supported-type systems containing nanosheets that exhibit C_2H_4 FEs between 50–80% can be identified, albeit without the intrinsic capability of the secondary particles for making C_2H_4. These systems include *e.g.*, CuO NPs supported on $CuSiO_3$ lamella[63] (52% C_2H_4), CuO_x NCs on Al_2O_3 nanosheets[70] (71% C_2H_4), CuO NPs on Al_2CuO_4 nanosheets[69] (79% C_2H_4), Cu/Pd mixed NPs supported on Bi_2S_3 nanosheets[121] (57% C_2H_4) and CuO_x NPs supported on Sm_2O_3 nanosheets[122] (49% C_2H_4). Importantly, the effect is not limited to only nanosheet-based supported-type systems, with Sn-doped CuO nanosheets,[123] Al-doped CuO_x nanosheets,[124] B-doped CuO

© 2025 The Author(s). Published by the Royal Society of Chemistry

Open Access Article. Published on 27 2025. Downloaded on 14-02-2026 07:37:44.
This article is licensed under a Creative Commons Attribution 3.0 Unported Licence.

'nanobundles' (composed of nanowires and nanosheets),[125] graphene oxide nanodots on CuO nanosheets[126] and Zn–Cu nanosheet arrays[127] all having been reported to exhibit maximum C_2H_4 FEs in the range of 50–60%. Finally, several truly excellent C_2H_4 electrocatalysts also consist of nanosheets, with defective Cu nanosheets,[5] alloyed hexagonal CuNi[128] nanosheets and alloyed hexagonal CuCo[129] nanosheets all exhibiting maximum C_2H_4 FEs of *ca.* 80%. Together, these results demonstrate the importance of the nanosheet morphology as a driver for high C_2H_4 selectivity.

Although the original publications do not report on this nanosheet effect nor its origin, we hypothesize that the trend might be related to the way that nanosheets stack – with the long sheets preventing intermediates from diffusing away rapidly. Hence, we are arguing for a nanoconfinement effect rather than specifically a nanosheet effect. To corroborate this hypothesis, we enumerate various non-nanosheet catalyst systems where we found the morphology to be especially conducive to trapping intermediates: CuO_x NPs trapped in a porous carbon matrix containing Ni-SAC sites,[130] yielding a maximum C_2H_4 FE of 72%; porous Cu_2O microparticles impregnated with a Co-based TMC,[43] generating 76% C_2H_4 both in the presence and absence of the cobalt complex; Cu-SAC sites dispersed within the nanopores of a cathodically stable Zr-based MOF,[131] making 62% C_2H_4; ordered CuO particles with a zeolite-like structure, coated with a $CuSiO_3$ layer,[132] giving a maximum C_2H_4 FE of 82%; a Cu/Ce bi-elemental catalyst with a hollow nanofiber morphology reported to make 78% C_2H_4;[133] and finally, a catalyst system consisting of copper sites decorating defective, hollow Au/Ag nanoframes[134] that can make up to 77% C_2H_4. These catalysts' morphologies are depicted in Fig. 2 and compared to the typical morphology for nanosheet-based catalysts as identified in this work.

Besides sharing a morphology that can effectively trap intermediates, the catalysts previously described and depicted in Fig. 2 all provide exceptionally high C_2H_4 selectivities. Because of this, we hypothesize that the morphological nanosheet effect stems from increased residence time of the intermediates through nanoconfinement effects.

2.4. Suppressed selectivity of tandem-type systems

In this section we discuss global observations relating to tandem-type catalyst systems, which we define herein as dual-component catalyst systems that contain a dedicated CO_2-to-CO conversion catalyst and a separate CO-to-C_2H_4 conversion catalyst. Considering the focus of this manuscript, our definition only pertains to systems where such catalysts pairs are present in a single device. Hence, the catalysts are generally (though not necessarily[136,137]) part of the same cathode, which means that the applied bias is equal for both the CO and C_2H_4 forming constituents. Because of this, aligning the catalysts' potential such that their respective optima for CO and C_2H_4 activity match is important for achieving good overall CO_2-to-C_2H_4 selectivity[138] in addition to matching the formation and depletion rates of CO through optimizing the relative loadings of the individual components. Many different materials are found to catalyze the electroconversion of CO_2 to CO,[139] including *e.g.*, Au,[140] Ag,[141] Zn[142] and Ni-SACs.[143,144] This high catalyst variability has resulted in the body of literature that we have identified and analyzed being quite extensive, benefitting the statistical significance of our findings.

From a holistic perspective, we find that most of these tandem-type catalyst systems yield maximum C_2H_4 FEs in the range of 50–60%. A small number of outliers exhibiting higher C_2H_4 selectivities were identified, but exactly those tandem-type systems were observed to have additional differentiating features that strongly correlated with their improved performance. To specify, various tandem-type electrocatalysts yielding $\geq$60% C_2H_4 also had nanoconfining morphological features such as *e.g.*, copper sites distributed on the ribs of CO-forming hollow Au/Ag nanoframes[134] (77% C_2H_4); CuO_x NPs distributed in the micropores of a carbon matrix containing CO-forming Ni-SAC sites[130] (72% C_2H_4); porous Cu_2O microparticles impregnated with a CO-forming Co-based TMC[43] (76% C_2H_4) and a Cu-SAC catalyst dispersed within the nanopores of a morphologically stable CO-forming Zr/Ir-based MOF[131] (71% C_2H_4). For those systems, we hypothesize it is the nanoconfinement effect that allows for their exceptional C_2H_4 selectivity as opposed to addition of the CO-forming component yielding extraordinary results. In part, this is substantiated by the results of the Cu_2O/Co-TMC system[43] and the Cu-SAC/Zr,Ir-MOF system,[131] for which very similar performance was obtained when CO was used as the reagent in absence of the CO-forming component.

Besides confounding nanoconfinement morphologies, several other high-selectivity tandem-type catalyst systems were identified to contain organic and/or inorganic constituents. Examples of such organic/inorganic additives include *e.g.*, polymeric coatings, addition of ionic liquids to the catalyst layer, thiol-bound surface modifying agents, PTFE coatings, cross-linked ionomer overlayers and carbon-derived overlayers. The presence of such (typically polymeric) components is often found to be beneficial for C_2H_4 selectivity such as reported by *e.g.*, Zhiji *et al.* for Cu paired with substituted pyridinium additives[145] and by Chen *et al.* for polyamine-incorporated Cu electrodes.[4] This effect is discussed in detail in a perspective by Nam *et al.*[146] wherein they label it the 'molecular enhancement effect', showing that various different products can be promoted depending on the specific nature of the molecular constituent. Importantly, all of the remaining tandem-type electrocatalysts that yield $\geq$60% C_2H_4 were found to contain such polymeric constituents, consisting of a Cu/Ag system where a Cu NP/Nafion layer was deposited on top of an Ag foil[147,148] (76% C_2H_4) and a Cu/Zn system modified with a Nafion/PVDF coating[149] (74% C_2H_4). In line with our nanoconfinement argument, we hypothesize that the exceptional C_2H_4 selectivity of these specific tandem-type systems is driven by the molecular enhancement effect rather than originating from the tandem action.

Our last observation regarding tandem-type systems is that they are absent from the best-performing C_2H_4 electrocatalysts ($\geq$70% C_2H_4 FE, Table 1) when we omit catalyst systems that are confounded with either nanoconfinement and/or polymeric/molecular enhancement effects. This absence of top-tier, purely

Open Access Article. Published on 27 2025. Downloaded on 14-02-2026 07:37:44.
This article is licensed under a Creative Commons Attribution 3.0 Unported Licence.

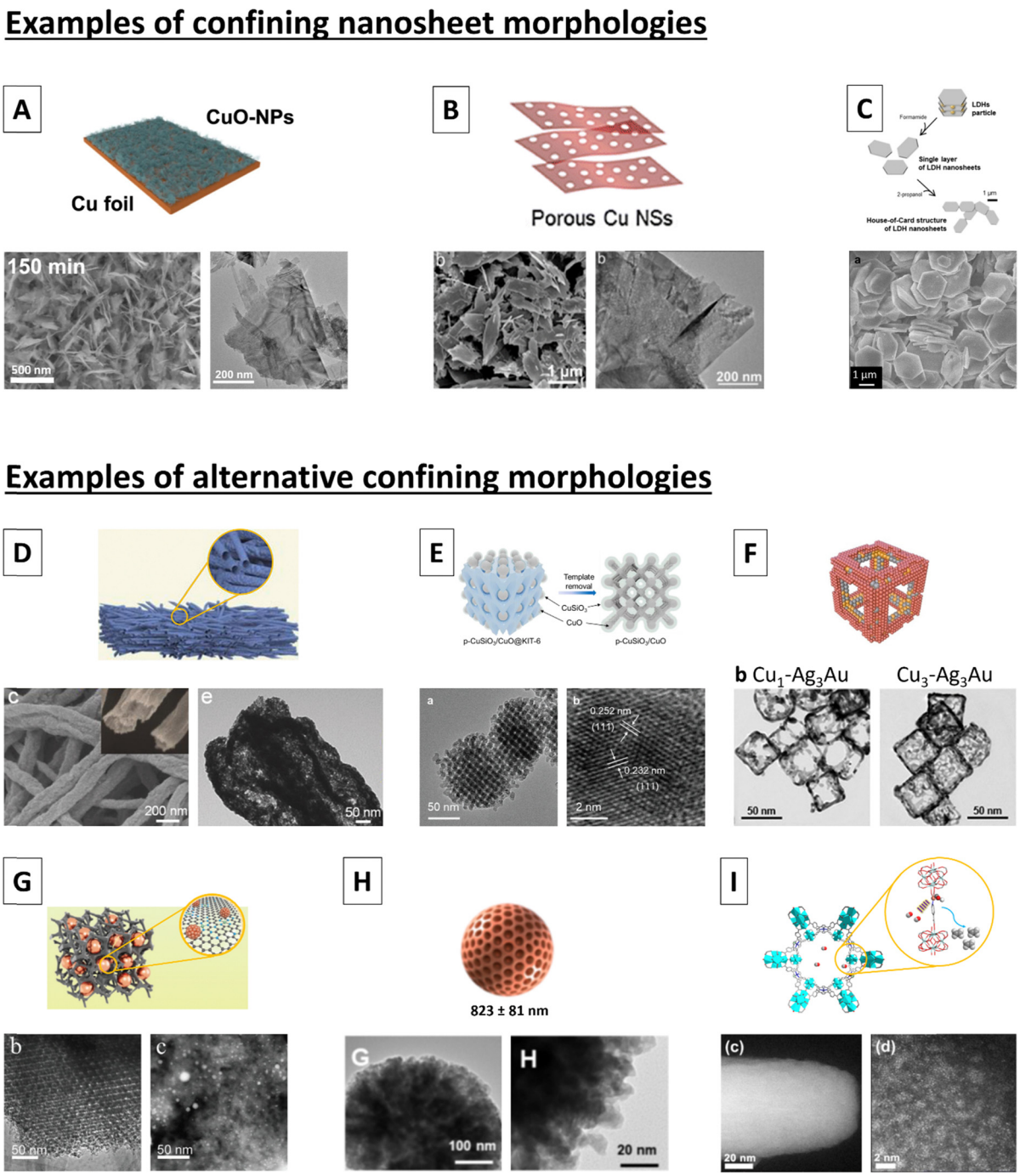

Fig. 2 (A)–(C) Morphologies of 2D nanosheet systems compared to (D)–(I) catalyst systems exhibiting nanoconfining morphologies as identified in this perspective. Individual sub-figures are adaptations from the following sources: A,[6] B,[135] C,[71] D,[133] E,[132] F,[134] G,[130] H,[43] I.[131]

tandem-type catalyst systems is noteworthy considering the large quantity of such types of systems present in the dataset. It seems that requiring the presence of two largely independent, though electrically connected, catalysts being located closely together in a single electrochemical cell is not necessarily beneficial to achieving higher C_2H_4 selectivities. However, we also find that the suppressed activity of tandem-type systems can be improved to a considerable degree by incorporating additional selectivity-enhancing features into the catalyst system, like the previously described confining morphologies or tuning the microenvironment through the addition of *e.g.*, polymeric components.

2.5. Polymeric (molecular) enhancement effect

Although we discussed enhanced C_2H_4 selectivity for specifically tandem-type systems having been modified with organic and/or inorganic constituents, we find that this effect is generalizable to other types of catalyst systems as well. For instance, we identified a Cu/Pb catalyst supported on a polyaniline-modified carbon

© 2025 The Author(s). Published by the Royal Society of Chemistry

Open Access Article. Published on 27 2025. Downloaded on 14-02-2026 07:37:44.
This article is licensed under a Creative Commons Attribution 3.0 Unported Licence.

substrate[150] that substantially out-performs other Cu/Pb systems. However, we observe that the effect is most common for metallic copper and/or oxide-derived copper catalyst systems that contain organic and/or inorganic additives. This is illustrated in Tables S25 and S26 (ESI†), wherein we have summarized catalyst systems consisting of a copper (oxide) core having an organic or inorganic coating/shell, and (oxide-derived) Cu catalysts that have been post-modified with an organic and/or inorganic overlayer, respectively. Although morphologically distinct, we believe the trends we observe for these two types of systems have the same origin. As such, we discuss them in unison.

Given the extensive dataset available to us, the effect is best illustrated quantitatively. In the case of copper and copper oxide systems modified with (in-)organic additives, we find that 31 out of 70 table entries (*ca.* 44%) exhibit C_2H_4 FEs of $\geq$55%. This is comparable to what we observe for metallic copper and oxide-derived copper catalysts, for which we find that a combined 104 out of 213 entries (*ca.* 49%) yield C_2H_4 FEs of $\geq$55%. However, when we focus on the proportion of top-performing catalysts ($\geq$70% C_2H_4) within the $\geq$55% segment, we observe that 13 out of 31 (*ca.* 42%) of Cu systems modified with organic and/or inorganic components exhibit excellent C_2H_4 selectivity whilst this ratio is substantially lower for 'generic' metallic copper and oxide-derived copper catalysts, at 24 out of 104 entries (*ca.* 23%). This statistical outperformance is retained when we instead compare to the >55% segment of the entirety of the dataset *sans* polymerically enhanced systems, for which we find that 55 out of 224 entries yield exceptional C_2H_4 selectivity (*ca.* 25%). Importantly, when we correct for the alkaline CO_2RR enhancement effect through omitting such systems from our analysis, the relative outperformance of organic/inorganic-assisted catalyst systems remains, though the differences become smaller. Specifically, 6 out of 17 (*ca.* 35%) *vs.* 13 out of 56 (*ca.* 23%) *vs.* 35 out of 122 (*ca.* 29%) of the systems have outstanding C_2H_4 selectivity in the case of catalyst systems with organic/inorganic additives, 'generic' copper and oxide-derived copper systems, and the entirety of the dataset excluding organic/inorganic-assisted systems, respectively. These results exemplify the beneficial, selectivity-enhancing effect that organic and/or inorganic additives can have with respect to C_2H_4 formation.

Many others have also reported on this effect,[4,145,146,151–156] out of which we would like to highlight a recent perspective by Song *et al.*[151] that we found to be highly informative. Due to the large number of chemically distinct possible additives, numerous explanations have been proposed to underly the molecular enhancement effect, including, but not limited to, (i) increased CO_2 adsorption capacity, (ii) activation of the CO_2 molecule, (iii) tuning of the local environment through *e.g.*, changing hydrophobicity, changing hydrogen bonding or changing the charge distribution near the surface or (iv) regulating mass transport properties through changing the (local) morphology, including creating a confining environment.[151] Though the exact mechanism might differ from system to system, the overall trend is an increase in C_2H_4 selectivity.

2.6. Importance of heterogeneity

Our last global observation is regarding the effect of catalyst heterogeneity for achieving selective C_2H_4 production. Compared to the previous topics, this concept is more difficult to substantiate. However, having investigated the body of literature reported in this study, we consider this concept to have sufficient scientific merit. The hypothesis that heterogeneity plays a role in enhancing C_2H_4 activity is based on a diverse, seemingly disjointed set of themes that were found to be relatively consistent across multiple catalyst systems, which we will discuss in this section. The themes are also graphically represented in Fig. 3, depicting the levers which were found to play a role in increasing system heterogeneity and, by association, C_2H_4 selectivity.

The first theme looks at heterogeneity from an atomic perspective, by observing that systems containing thermodynamically unstable oxidation states have increased heterogeneity on account of such unstable sites typically being (i) randomly distributed, (ii) having highly variable (local) electron densities and (iii) having an ill-defined lifetime considering they exist in a state from which they could quickly transition into a different, chemically more stable state. Holistically, we observe that these heterogeneous systems comprising thermodynamically unstable oxidation states tend to outperform fully reduced catalyst systems. This topic has been debated in literature extensively and is included as a theme predominantly on account of its prominence in literature on copper-based catalyst systems, though it is also evident from oxide-derived copper studies. Many of those copper-based catalyst studies provide *in situ* results that show copper to exist in a partially oxidized state under (cathodic) operating conditions, which is typically found to persist for longer upon the addition of the co-element studied.[48,66,157–161] Often, this effect is hypothesized to be related to the (temporary) existence of a Cu^+ oxidation state,[157,158,162,163] similar to what is reported for oxide-derived Cu systems.[164,165] Importantly, these same studies also typically report that the *CO coverage is increased concomitantly.

The second theme looks at heterogeneity more from a morphological perspective, observing that catalyst systems with large quantities of (different types of) defects, especially when in the form of 2D surfaces, oftentimes exhibit excellent C_2H_4 selectivities. This superior catalytic performance is hypothesized to be grounded in the need for a variety of catalytic sites. For example, Scholten *et al.* have shown that a shortage of defect sites severely inhibits the C–C coupling reaction[166] whilst Kim *et al.* show that diversified surface sites aid in catalysis even if not catalytically active themselves through acting as a reservoir of readily accessible CO that is converted by the actual active sites into C_2H_4.[47] In addition, if large numbers of defects are introduced through leaching away material (as is often done), holes[5] and pores[43] are formed in 2D and 3D structures, respectively. Besides introducing numerous defect sites, such methods also yield complicated geometries that effectively trap intermediate species, which, as we discussed previously, can also enhance C_2H_4 selectivity.

A third reoccurring theme in favor of heterogeneity pertains to the importance of the local nano-environment, where we observe that close contact between chemically distinct sites yields enhanced C_2H_4 activity *vs.* simple physical mixing of components.[91,134,167–173] Heterogeneity of such systems is

Open Access Article. Published on 27 2025. Downloaded on 14-02-2026 07:37:44.
This article is licensed under a Creative Commons Attribution 3.0 Unported Licence.

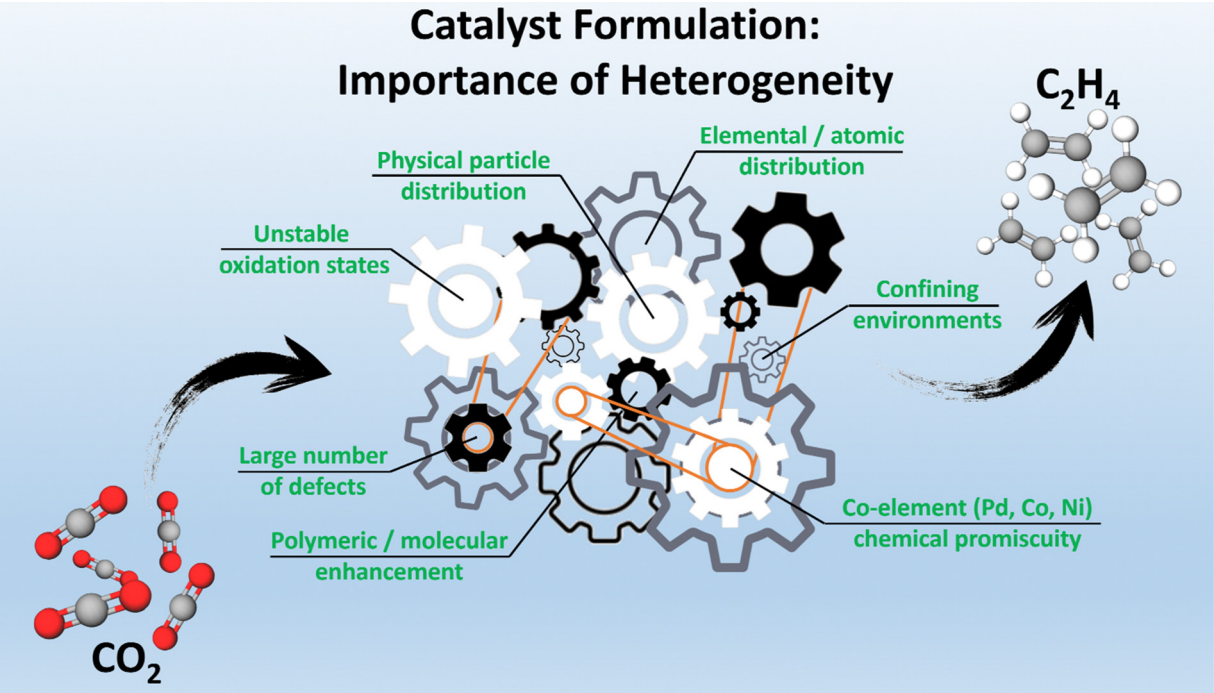

Fig. 3 Themes centered around catalyst heterogeneity that were identified to be beneficial for C_2H_4 selectivity.

increased as additional, intermediate chemical states become viable when chemically distinct species are in direct contact through (partial) charge transfer. The benefit of an intimate interface was demonstrated in a study by Sichao *et al.* who showed that C–C coupling was significantly enhanced for phase-separated Cu/Pd NPs compared to both ordered and disordered alloyed Cu/Pd NPs.[174] The fourth theme is similar to the third, and concerns the observation that a non-uniform distribution of non-equal elements yields improved catalytic activity *vs.* a homogeneous elemental distribution, an effect that is commonly reported for *e.g.*, core/shell-type systems (multi-phase catalyst systems consisting of a core comprised of material A wrapped with a chemically distinct shell comprised of material B),[175] and systems in which small amounts of (nonuniformly distributed) dopants are present – typically at the surface.[123,176–179]

The last theme in favor of heterogeneity is based on the observation that, out of the bi-elemental catalysts, Cu/Ni, Cu/Pd and Cu/Co systems seem to make for some of the best C_2H_4 electrocatalysts reported to date. When considered independently of copper, Ni, Pd and Co share a notable property, which is that they exhibit a wide range of possible CO_2RR chemistries besides high C_2H_4 selectivity; a characteristic we denote 'chemical promiscuity'. For example, Ni-based SACs make for superb CO forming catalysts,[143] whereas metallic Ni has been reported to make minor quantities of CH_4 and C_2H_4 in addition to H_2.[81,87,180] By contrast, nickel phosphides have been reported to make complex $C_{3\text{-}4}$ oxygenates[181] and acetone[18] as well as various other products.[182] Pd exhibits a similarly broad product spectrum,[183] being capable of selective HCOOH[184,185] and CO[186] production when coupled with non-Cu metals, and yielding *e.g.*, methanol,[187] acetate[174] and propanol[188] when coupled with Cu. In turn, Co[189] has been shown to be able to selectively produce CO[190] and HCOOH[191] in addition to C–C coupled products such as *e.g.*, ethanal[19,192] and EtOH[193] depending on the exact catalyst composition. This capacity of making a range of carbon-based and carbon-coupled electroreduction products is relatively uncommon, as most electrocatalysts (with the exception of Cu) are traditionally categorized as being either H_2, CO or HCOOH-forming.[194] We posit that these elements' varied chemistry denotes their adaptability, being able to vary their chemical properties to a sufficiently large degree to facilitate various different chemistries, *e.g.*, heterogeneity in the form of their chemical promiscuity.

Although the concept of heterogeneity might seem disproportionally correlated with the superior C_2H_4 selectivity of oxide-derived Cu catalysts, it is more broadly applicable. This is best illustrated by looking at the most selective catalyst systems identified in this study (C_2H_4 FEs $\geq$70%), which are listed in Table 1. We find that metallic and oxide-derived copper systems make up roughly a third (24/68) of the entries in the table, with this ratio largely unchanged if we omit alkaline CO_2RR systems from the comparison, at 13/41 entries. The other two-thirds comprise systems wherein additional components are present, either in the form of organic and/or inorganic modifying agents, or in the form of co-element(s). We use this observation as our last argument in favor of system heterogeneity as a driver for C_2H_4 performance. We posit that the heterogeneity effect predominantly improves selectivity through modulating the local environment, optimizing both the adsorption strengths of intermediates at the catalyst sites as well as the availability of intermediates near, and transportation of intermediates to, these

© 2025 The Author(s). Published by the Royal Society of Chemistry

Open Access Article. Published on 27 2025. Downloaded on 14-02-2026 07:37:44. This article is licensed under a Creative Commons Attribution 3.0 Unported Licence.

active sites. Clearly, more direct and unambiguous evidence for this hypothesis would be highly desirable, as it impacts on the way we "rationally design" optimal catalysts.

Looking at the catalyst systems described in Table 1, we find that it seems feasible to achieve FEs for C_2H_4 of at least 75–80% in an industrial setting. Indeed, various authors have reported independently on (diverse) catalyst systems with FEs in the low 80 s at applied current densities of $\geq|-150|$ mA cm^{-2} under reaction conditions where parasitic carbonate losses are not a concern.[128,129,195] Although publications reporting even higher FEs ($\geq$90%) have been reported by a single group for various catalytic systems,[42,127,196] these studies were conducted at low current densities (*i.e.*, $\leq|-10|$ mA cm^{-2}). Because of this, we are hesitant to declare such high FEs to be industrially feasible, though the results look promising. Albeit exhibiting slightly lower C_2H_4 selectivities, the rest of the catalyst systems described in Table 1[197–223] are noteworthy in their own right but describing them in more detail is not feasible in the current work.

2.7. Absence of alignment between studies

Although a large amount of knowledge was obtained from the publications analyzed herein, the overall learnings have been limited. We observe that heterogeneity, this time in the form of differences across publications, plays a substantial part in this. Because of this, we posit that improved standardization would benefit the field. Various factors contribute to the inhomogeneity of the results, including:

- Reactant type (CO_2 *vs.* CO).
- Mass transport properties (dissolved gas *vs.* gaseous, electrolyte flow *vs.* stirring *vs.* static).
- Membrane type (absent, diaphragm, cation-exchange, anion-exchange, bipolar).
- Temperature and temperature control (uncontrolled, electrolyte heating, cell heating).
- Pressure and pressure control (uncontrolled, back pressure regulated, with internal standard(s) present).
- Substrate type (*e.g.*, plates, foams, gas diffusion layers (GDLs)) and substrate elemental composition.
- The choice of electrolyte and its compatibility with the reactant.
- The way in which the data are reported (*e.g.*, in the form of graphs without exact numbers, in individual tables and/or summation tables, or as current efficiencies and/or partial current densities).

As described previously, many factors are important in determining the industrial applicability of a particular catalyst system for the electroformation of C_2H_4. However, most of these metrics (*e.g.*, maximum achievable current densities, overall energetic costs, system lifetime) necessitate investigating an optimized system, which is generally beyond the scope of scientific literature. As such, we do not advocate for scientific studies to provide industry these metrics (although this would certainly be beneficial). Instead, what we have identified to be missing from existing literature regarding $CO_{(2)}$RR electrocatalyst development is data comparability, data reproducibility and independent party result replication.

A strong contributor to the difficulties related with inter-publication comparability and result reproducibility is the diversity of electrolyzer systems used across studies, or rather, the effect that cell design has on mass transport properties. Two broad categories of electrolyzers exist: H-cell systems and gas diffusion electrode (GDE) systems. Depending on which type is used, the reactant is supplied either in the dissolved state (H-cell systems) or in the gaseous state (GDE systems). Although various sub-configurations exist, such as *e.g.*, which type of support employed, how gases flow through the system and how water is supplied to the interfaces, the main differentiating factor is mass transport characteristics. Previous works by Chae *et al.*[224] and Tan *et al.*,[225] detail the extent to which the resulting differences in mass transport properties influence the measurement outcome for an otherwise identical catalyst. One way to prove the absence of mass transport limitations in a study could be by reporting the CORR activity alongside the CO_2RR activity, considering that the much poorer solubility of CO *vs.* CO_2 (1 mM *vs.* 33 mM) would significantly worsen mass transportation issues. *E.g.*, Bernasconi *et al.* use this concept to show that their GDE system does not actually form a 3-phase reaction interface.[226] Guaranteeing the reliability of results and ensuring reproducibility across institutes necessitates proving that the measurements were conducted in the absence of mass transportation limitations. From an industrial perspective, we are strongly in favor of using GDE systems as they not only significantly reduce the chances of running into mass transportation limited regimes, but also enable operation at industrially relevant current densities.

A second factor that limits inter-study comparability and reproducibility is the difference in (and absence of) control of process conditions. These process conditions include *e.g.*, (partial) pressure control, temperature control and means of electrolyte delivery and agitation. These process conditions are often not reported, and thus (presumably) not actively measured nor controlled. However, they can fluctuate considerably depending on the local laboratory conditions, exact operating conditions, and the type of electrolyzer employed. Importantly, variations in these process conditions will significantly influence the product distribution, as has been reported for *e.g.*, temperature[40,227,228] and feedstock conversion level[40] (by way of the reactant's (partial[229–231]) pressure[220,232,233]). As such, we consider it a necessity to at least measure and report these process conditions. However, we firmly believe a good measurement involves actively controlling them, such that fluctuations in the operating conditions (*e.g.*, current density, cell voltage) do not result in significant changes in the process conditions.

The third consideration is regarding the lack of a standardized catalyst that can be used as a benchmark to prove the validity of the electrolyzer setup. Although a generic copper catalyst is often included, there is too much variation in its performance on account of differences in *e.g.* morphology, crystallographic orientation, particle size and size distribution. In addition, GDE manufacturing methodologies and employed substrates can vary significantly, resulting in large variation in catalytic performance. Therefore, we strongly argue that a well-documented, easily obtainable, and affordable catalyst with

Open Access Article. Published on 27 2025. Downloaded on 14-02-2026 07:37:44.
This article is licensed under a Creative Commons Attribution 3.0 Unported Licence.

thoroughly verified performance is required. Likely, the best candidate would be a catalyst that can be made in every lab without the need of extreme conditions or expensive equipment. Although various such catalysts are reported in the papers that make up the dataset described in this perspective, we are of the opinion that a full-fledged study regarding the identification of a robust benchmark catalyst would be of great benefit to the field. Such a study might involve *e.g.*, identifying affordable and reproducible means to synthesize copper nanoparticles, which are subsequently turned into GDEs (and possibly other types of electrodes) *via* specific, well-documented procedures employing off-the-shelf components, and then have their performance and performance reproducibility investigated under standardized (and actively controlled) conditions. Preferably a brief durability test would also be included, such that authors who adopt this standardized testing methodology could identify possible time-dependent problems their local setup might have.

Besides significant inter-study electrolyzer variability, a lack of control and quantification of important process conditions and the unavailability of a stable, well-defined, and reproducible baseline catalyst system, we also identified the absence of standardized measurement protocols as an additional factor in the poor reproducibility of results across research groups. To draw a parallel with the more mature field of solar cells, a large amount of effort was dedicated to establishing such so-called consensus performance testing protocols.[234–236] In part, the absence of these types of protocols in the field of $CO_{(2)}$ electrolysis can be explained by the relative immaturity of the field in concert with the increased complexity of $CO_{(2)}$RR measurements in general. Although it is evident from other fields that such protocols are an important component in facilitating reproducibility and measurement reliability, it is difficult to adapt field-specific protocols (such as available for solar cells) to a different field, instead necessitating a bottom-up approach in developing such protocols although inspiration can be taken from other fields.

For the field of CO_2RR to be able to accelerate, we posit that a minimum of standardization must be implemented so-as to enable objective comparison of research outputs between different groups. Taking inspiration from the field of solar cells, establishing such consensus protocols requires the inputs of numerous independent researchers to be refined into a set of concrete steps regarding which sets of experiments need to be conducted at a minimum, and how to conduct them. Organizing focus group discussions with prominent experts in the field such as during *e.g.*, international field-relevant conferences seems to be a viable route to establishing such protocols.[236] Importantly, such a minimum protocol should not exclude research groups based on their financial capability whilst still allowing for measurement results to be compared like-for-like through systemic instructions on which parameters to assess, how to determine them, and how to prove and/or guarantee the validity of the results.

A final issue pertains to the absence of result verification by independent parties. At this moment, <5 of the studies we discuss in this perspective (out of many hundreds) have had their results tested by a third party. Periodically validating the top-performing newly identified catalysts in a systemic manner at an identical workstation would be of significant value to industry, but also to the field at large. An invited publication could be employed to assure that such a practice becomes implemented. We are of the opinion that such a practice would be highly beneficial to the development of CO_2 to ethylene electrocatalysts.

2.8. Facilitating industrial relevancy

Although we do not advocate for scientific catalyst studies to directly provide all parameters that are relevant for industry, minor changes can be implemented to improve a work's industrial relevance. Foremost, we advocate for reporting tabulated Faraday efficiency data on a per-product basis for all measurements discussed in the manuscript, including total FEs, current densities and applied overpotentials together with measured cathode-reference electrolyte resistance values, if available. The difficulty associated with accurately comparing results across research groups with respect to non-tabular formats is illustrated in Fig. 4, wherein common graphical representations are illustrated for which extracting accurate FEs is non-trivial/time consuming. Secondly, we advocate for including a brief durability measurement. Although we previously argued that estimating industrially relevant catalyst lifetime necessitates investigating a fully optimized system, an initial indication of lifetime can be obtained with much less effort without the need for a fully optimized system. Arguably, measuring short-term performance benefits from being conducted in a standardized system instead of an optimized system, making it more scientifically feasible. We advocate for measuring performance stability over a period of minimally 12 h, but preferably $\geq$100 h as certain effects are only observable on longer timescales.[38,237,238] In addition, the time-dependent performance should be compared to the behavior of a standardized catalyst measured under otherwise identical conditions to prove that intrinsic catalyst stability is measured rather than auxiliary degradation processes. Although such a durability measurement does not provide much insight into industrial applicability nor catalyst behavior under industrial conditions for prolonged periods of time, it will provide valuable information about the system and the catalyst itself.[239] For further information, we direct the reader to a dedicated review on the topic of stability during CO_2 electrolysis.[240]

A final set of industrially relevant measurements that can be implemented with reasonable ease are regarding catalyst optimization. Catalyst layer thickness (*i.e.*, loading), catalyst-to-ionomer ratio, partial reactant pressure, temperature and electrolyte composition have all been shown to have a significant impact on electrocatalytic performance. Ideally, one would compare catalyst performance trends as a function of all these parameters to be able to rigorously assess which catalyst is objectively better than another. Reporting performance under a range of different (standardized) conditions as determined by *e.g.* a design of experiment (DoE) approach would yield a more complete picture of catalyst performance and allow for mathematically sound data interpolation to ascertain the conditions where maximum performance is achieved.

© 2025 The Author(s). Published by the Royal Society of Chemistry

Open Access Article. Published on 27 2025. Downloaded on 14-02-2026 07:37:44.
This article is licensed under a Creative Commons Attribution 3.0 Unported Licence.

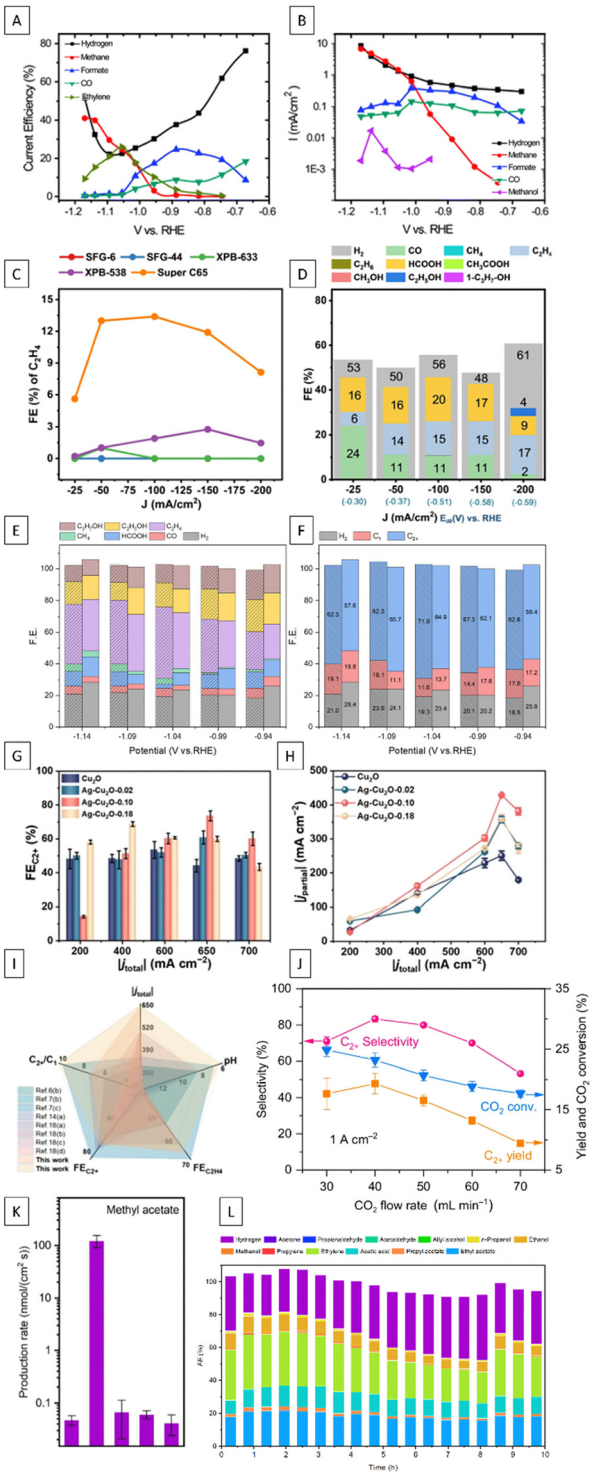

Fig. 4 Various types of graphical reporting styles that increase the difficulty of inter-study result comparison. Individual sub-figures were adapted with permission from the following sources: A & B,[241] C & D,[242] E & F,[243] G, H & I,[244] J,[165] K & L.[245]

Although experimentally intensive, investigating the effect of many different variables simultaneously allows for experiment optimization through partial factorial design, significantly reducing the experimental burden. If this would be implemented by default (*e.g.*, for the best-performing catalyst in a study), comparing different publications becomes both easier and more meaningful.

3. Conclusions/outlook

In this study, we sought to identify global trends with respect to favorable catalyst properties and/or characteristics for achieving high C_2H_4 selectivity from electrochemical $CO_{(2)}$ reduction on copper-based catalysts. High C_2H_4 selectivity is what we consider to be the best indicative descriptor of potential industrial applicability. We investigated approximately 630 publications reporting on >850 copper-based catalyst systems exceeding a pre-defined C_2H_4 FE threshold and extracted 6 global trends that reoccur across many catalyst systems with highly varied chemical and morphological characteristics.

Specifically, we found that (trend 1) tandem-type and (trend 2) supported-type systems yield suppressed C_2H_4 selectivity compared to other catalyst systems: *ca.* 50–60% C_2H_4 *vs.* ≥70%. However, the C_2H_4 selectivity of such tandem- and supported-type systems can be improved by (i) implementing confining morphologies, (ii) adding polymeric constituents and/or (iii) employing chemically modified forms of carbon (for supported-type systems). Overall, we conclude that supported-type systems have greater potential than tandem-type systems for industrial application on account of higher demonstrated C_2H_4 selectivities with an arguably simpler system considering there is no need to match potentials between two distinct catalyst species nor to match catalyst loadings such that reaction rates are aligned.

To continue, we found that catalysts with a nanosheet morphology exhibit above-average C_2H_4 selectivities (trend 3), which we attribute to the nanoconfining morphology originating from the stacking of these nanosheets. We expand this reasoning to other systems, showing that morphologies conducive to intermediate trapping can yield excellent C_2H_4 selectivities. We also identified that organic and/or inorganic modifying agents can substantially increase C_2H_4 selectivity (trend 4), in line with established literature.[4,145,146,151–156] The next trend (trend 5) concerns the observation that heterogeneity is important for obtaining selective C_2H_4 formation, as evidenced by the large differences between top-performing (≥70% C_2H_4, Table 1) catalyst systems. Overall, we conclude that optimizing the microenvironment is vital for achieving high C_2H_4 selectivity.

Lastly (trend 6) we observe that both CO_2 and CO can be used as a feedstock with little effect on maximum achievable C_2H_4 performance, applying to metallic and oxide-derived Cu catalysts in general, and to copper-based catalyst systems exhibiting ≥70% FEs for C_2H_4. This is beneficial from an industrial perspective on account of increased freedom in designing process lineups involving CO_2- and CO-reducing electrolyzers.

Although the discussed dataset is comprehensive, we found that a lack of standardization and control of process conditions hindered the learnings that could be extracted. For example, although several independent groups have achieved 75–80% C_2H_4 for chemically distinct catalyst systems under industrially relevant current densities, most of these catalyst systems'

Open Access Article. Published on 27 2025. Downloaded on 14-02-2026 07:37:44.
This article is licensed under a Creative Commons Attribution 3.0 Unported Licence.

performances have not been replicated to date. We conclude that reproducibility and a lack of independent result verification is currently a setback for this field. Therefore, we advocate for a thorough study that focuses on identifying, characterizing and rigorously assessing the performance of a simple catalyst system that can be used as a benchmark material across research groups. Also, standardized measurement protocols in line with what is available for more mature electrochemical subdomains such as solar cells need to be developed, ideally including periodic replication of top-performing systems by independent parties. Finally, we discuss various strategies for increasing the industrial relevancy of electrocatalyst-focused research projects.

We propose that next steps should involve investigating the energy efficiencies, lifetime, and behavior under reactant-constrained conditions (*i.e.*, high single-pass conversion rates) of the catalyst systems with the highest C_2H_4 selectivities described in this work. A follow-up should also include assessing whether the global C_2H_4 performance-enhancing trends discussed within this article can be combined to further optimize the selectivity of electrocatalysts with high intrinsic catalytic activity. Our findings provide a framework for designing robust and reproducible electrocatalysts with increased C_2H_4 selectivity, propelling the realization of $CO_{(2)}$RR technology at industrial scales. The implementation of this technology at an industrial level will allow for reducing the carbon footprint of the molecules and materials in use today with minimal changes to existing industrial infrastructure and chemical processes, provided that the required $CO_{(2)}$ and (electrical) energy are procured from non-fossil sources.

Author contributions

Stefan J. Raaijman: conceptualization, data curation, formal analysis, investigation, visualization, writing – original draft, writing – review & editing. Maarten P. Schellekens: conceptualization, data curation, formal analysis, investigation, visualization, writing – original draft. Yoon Jun Son: visualization. Marc T. M. Koper: conceptualization, validation, writing – review & editing, supervision. Paul J. Corbett: conceptualization, formal analysis, funding acquisition, project administration, resources, supervision, validation, visualization, writing – review & editing.

Data availability

The data supporting this article have been included as part of the ESI.†

Conflicts of interest

There are no conflicts to declare.

Acknowledgements

We would like to thank our colleagues Ben Rowley and Kai Han of Shell Global Solutions International B.V. for sending relevant publications our way.

Notes and references

1 Y. Cui, C. Kong, C. Yang, Y. Su, Y. Cheng, D. Yao, G. Chen, K. Song, Z. Zhong, Y. Song, G. Wang, Z. Li and L. Zhuang, *ACS Catal.*, 2023, **13**, 11625–11633.
2 X. Zhou, J. Shan, L. Chen, B. Y. Xia, T. Ling, J. Duan, Y. Jiao, Y. Zheng and S.-Z. Qiao, *J. Am. Chem. Soc.*, 2022, **144**, 2079–2084.
3 Y. Zheng, Y. Wang, Y. Yuan and H. Huang, *ChemNanoMat*, 2021, **7**, 502–514.
4 X. Chen, J. Chen, N. M. Alghoraibi, D. A. Henckel, R. Zhang, U. O. Nwabara, K. E. Madsen, P. J. A. Kenis, S. C. Zimmerman and A. A. Gewirth, *Nat. Catal.*, 2021, **4**, 20–27.
5 B. Zhang, J. Zhang, M. Hua, Q. Wan, Z. Su, X. Tan, L. Liu, F. Zhang, G. Chen, D. Tan, X. Cheng, B. Han, L. Zheng and G. Mo, *J. Am. Chem. Soc.*, 2020, **142**, 13606–13613.
6 W. Liu, P. Zhai, A. Li, B. Wei, K. Si, Y. Wei, X. Wang, G. Zhu, Q. Chen, X. Gu, R. Zhang, W. Zhou and Y. Gong, *Nat. Commun.*, 2022, **13**, 1877.
7 N. Zhu, X. Zhang, P. Wang, N. Chen, J. Zhu, X. Zheng, Z. Chen, T. Sheng and Z. Wu, *ACS Sustainable Chem. Eng.*, 2024, **12**, 2969–2977.
8 K. D. Yang, W. R. Ko, J. H. Lee, S. J. Kim, H. Lee, M. H. Lee and K. T. Nam, *Angew. Chem., Int. Ed.*, 2017, **129**, 814–818.
9 M. Esmaeilirad, Z. Jiang, A. M. Harzandi, A. Kondori, M. Tamadoni Saray, C. U. Segre, R. Shahbazian-Yassar, A. M. Rappe and M. Asadi, *Nat. Energy*, 2023, **8**, 891–900.
10 G. Wu, C. Zhu, J. Mao, G. Li, S. Li, X. Dong, A. Chen, Y. Song, G. Feng, X. Liu, Y. Wei, J. Wang, W. Wei and W. Chen, *ACS Energy Lett.*, 2023, **8**, 4867–4874.
11 B.-B. Zhang, Y.-H. Wang, S.-M. Xu, K. Chen, Y.-G. Yang and Q.-H. Kong, *RSC Adv.*, 2020, **10**, 19192–19198.
12 K. A. Adegoke, S. G. Radhakrishnan, C. L. Gray, B. Sowa, C. Morais, P. Rayess, E. R. Rohwer, C. Comminges, K. B. Kokoh and E. Roduner, *Sustainable Energy Fuels*, 2020, **4**, 4030–4038.
13 J. Ding, H. Bin Yang, X.-L. Ma, S. Liu, W. Liu, Q. Mao, Y. Huang, J. Li, T. Zhang and B. Liu, *Nat. Energy*, 2023, **8**, 1386–1394.
14 W. Niu, Z. Chen, W. Guo, W. Mao, Y. Liu, Y. Guo, J. Chen, R. Huang, L. Kang, Y. Ma, Q. Yan, J. Ye, C. Cui, L. Zhang, P. Wang, X. Xu and B. Zhang, *Nat. Commun.*, 2023, **14**, 4882.
15 X. Wang, P. Ou, A. Ozden, S.-F. Hung, J. Tam, C. M. Gabardo, J. Y. Howe, J. Sisler, K. Bertens, F. P. García de Arquer, R. K. Miao, C. P. O'Brien, Z. Wang, J. Abed, A. S. Rasouli, M. Sun, A. H. Ip, D. Sinton and E. H. Sargent, *Nat. Energy*, 2022, **7**, 170–176.
16 H. Phong Duong, J. G. Rivera de la Cruz, N.-H. Tran, J. Louis, S. Zanna, D. Portehault, A. Zitolo, M. Walls, D. V. Peron, M. W. Schreiber, N. Menguy and M. Fontecave, *Angew. Chem., Int. Ed.*, 2023, e202310788.
17 C. Long, K. Wan, Y. Chen, L. Li, Y. Jiang, C. Yang, Q. Wu, G. Wu, P. Xu, J. Li, X. Shi, Z. Tang and C. Cui, *J. Am. Chem. Soc.*, 2024, **146**, 4632–4641.
18 M.-G. Kim, Y. Choi, E. Park, C.-H. Cheon, N.-K. Kim, B. K. Min and W. Kim, *ACS Appl. Energy Mater.*, 2020, **3**, 11516–11522.

© 2025 The Author(s). Published by the Royal Society of Chemistry

Open Access Article. Published on 27 2025. Downloaded on 14-02-2026 07:37:44. This article is licensed under a Creative Commons Attribution 3.0 Unported Licence.

19 J. Yin, Z. Yin, J. Jin, M. Sun, B. Huang, H. Lin, Z. Ma, M. Muzzio, M. Shen, C. Yu, H. Zhang, Y. Peng, P. Xi, C.-H. Yan and S. Sun, *J. Am. Chem. Soc.*, 2021, **143**, 15335–15343.
20 K. Zhao, X. Nie, H. Wang, S. Chen, X. Quan, H. Yu, W. Choi, G. Zhang, B. Kim and J. G. Chen, *Nat. Commun.*, 2020, **11**, 2455.
21 L. Wang, D. C. Higgins, Y. Ji, C. G. Morales-Guio, K. Chan, C. Hahn and T. F. Jaramillo, *Proc. Natl. Acad. Sci. U. S. A.*, 2020, **117**, 12572–12575.
22 A. Ostovari Moghaddam, S. Mehrabi-Kalajahi, A. Abdollahzadeh, R. Salari, X. Qi, R. Fereidonnejad, S. A. Akaahimbe, M. Nangir, D. A. Uchaev, M. A. Varfolomeev, A. Cabot, A. S. Vasenko and E. A. Trofimov, *J. Phys. Chem. Lett.*, 2024, **15**, 5535–5542.
23 P. T. Anastas and J. C. Warner, *Green chemistry: theory and practice*, Oxford University Press, 2000.
24 M. Jouny, W. Luc and F. Jiao, *Ind. Eng. Chem. Res.*, 2018, **57**, 2165–2177.
25 J. M. Spurgeon and B. Kumar, *Energy Environ. Sci.*, 2018, **11**, 1536–1551.
26 H. Shin, K. U. Hansen and F. Jiao, *Nat. Sustain.*, 2021, **4**, 911–919.
27 G. Leonzio, A. Hankin and N. Shah, *Chem. Eng. Res. Des.*, 2024, **208**, 934–955.
28 C.-T. Dinh, T. Burdyny, M. G. Kibria, A. Seifitokaldani, C. M. Gabardo, F. P. García de Arquer, A. Kiani, J. P. Edwards, P. De Luna, O. S. Bushuyev, C. Zou, R. Quintero-Bermudez, Y. Pang, D. Sinton and E. H. Sargent, *Science*, 2018, **360**, 783–787.
29 R. L. Cook, R. C. MacDuff and A. F. Sammells, *J. Electrochem. Soc.*, 1990, **137**, 607–608.
30 T. Alerte, J. P. Edwards, C. M. Gabardo, C. P. O'Brien, A. Gaona, J. Wicks, A. Obradović, A. Sarkar, S. A. Jaffer, H. L. MacLean, D. Sinton and E. H. Sargent, *ACS Energy Lett.*, 2021, **6**, 4405–4412.
31 W. Fang, W. Guo, R. Lu, Y. Yan, X. Liu, D. Wu, F. M. Li, Y. Zhou, C. He, C. Xia, H. Niu, S. Wang, Y. Liu, Y. Mao, C. Zhang, B. You, Y. Pang, L. Duan, X. Yang, F. Song, T. Zhai, G. Wang, X. Guo, B. Tan, T. Yao, Z. Wang and B. Y. Xia, *Nature*, 2024, **626**, 86–91.
32 A. Pătru, T. Binninger, B. Pribyl and T. J. Schmidt, *J. Electrochem. Soc.*, 2019, **166**, F34.
33 X. She, L. Zhai, Y. Wang, P. Xiong, M. M.-J. Li, T.-S. Wu, M. C. Wong, X. Guo, Z. Xu, H. Li, H. Xu, Y. Zhu, S. C. E. Tsang and S. P. Lau, *Nat. Energy*, 2024, **9**, 81–91.
34 T. Zhang, J. Zhou, T. Luo, J.-Q. Lu, Z. Li, X. Weng and F. Yang, *Chem. – Eur. J.*, 2023, **29**, e202301455.
35 H. Zimmermann and R. Walzl, *Ullmann's Encyclopedia of Industrial Chemistry*, Wiley-VCH Verlag GmbH & Co. KGaA, 7th edn, 2011, vol. 13, pp. 465–529.
36 N. Kosaric, Z. Duvnjak, A. Farkas, H. Sahm, S. Bringer-Meyer, O. Goebel and D. Mayer, *Ullmann's Encyclopedia of Industrial Chemistry*, 2011, pp. 1–72, DOI: **10.1002/14356007.a09_587.pub2**.
37 Y. Sun, F. Bai, J. Liu, S. Sun, Y. Mao, X. Liu, Y. Huang and Y. Chen, *J. Phys. Chem. Lett.*, 2024, **15**, 9122–9128.
38 B. Sahin, S. Kimberly Raymond, F. Ntourmas, R. Pastusiak, K. Wiesner-Fleischer, M. Fleischer, E. Simon and O. Hinrichsen, *ACS Appl. Mater. Interfaces*, 2023, **15**, 45844–45854.
39 A. J. Martín, G. O. Larrazábal and J. Pérez-Ramírez, *Green Chem.*, 2015, **17**, 5114–5130.
40 M. P. Schellekens, S. J. Raaijman, M. T. M. Koper and P. J. Corbett, *Chem. Eng. J.*, 2024, **483**, 149105.
41 C. Choi, S. Kwon, T. Cheng, M. Xu, P. Tieu, C. Lee, J. Cai, H. M. Lee, X. Pan, X. Duan, W. A. Goddard and Y. Huang, *Nat. Catal.*, 2020, **3**, 804–812.
42 I. Merino-Garcia, J. Albo and A. Irabien, *Nanotechnology*, 2018, **29**, 014001.
43 Y. Wang, Q. Cheng, H. Zhang, L. Ma and H. Yang, *Chem. Eng. J.*, 2024, **492**, 152254.
44 H. P. Duong, N.-H. Tran, G. Rousse, S. Zanna, M. W. Schreiber and M. Fontecave, *ACS Catal.*, 2022, **12**, 10285–10293.
45 R. Wang, J. Liu, L.-Z. Dong, J. Zhou, Q. Huang, Y.-R. Wang, J.-W. Shi and Y.-Q. Lan, *CCS Chem.*, 2023, **5**, 2237–2250.
46 Y. Jiang, X. Wang, D. Duan, C. He, J. Ma, W. Zhang, H. Liu, R. Long, Z. Li, T. Kong, X. J. Loh, L. Song, E. Ye and Y. Xiong, *Adv. Sci.*, 2022, **9**, 2105292.
47 C. Kim, N. Govindarajan, S. Hemenway, J. Park, A. Zoraster, C. J. Kong, R. R. Prabhakar, J. B. Varley, H.-T. Jung, C. Hahn and J. W. Ager, *ACS Catal.*, 2024, **14**, 3128–3138.
48 M. Xie, Y. Shen, W. Ma, D. Wei, B. Zhang, Z. Wang, Y. Wang, Q. Zhang, S. Xie, C. Wang and Y. Wang, *Angew. Chem., Int. Ed.*, 2022, **61**, e202213423.
49 H. Bao, Y. Qiu, X. Peng, J.-A. Wang, Y. Mi, S. Zhao, X. Liu, Y. Liu, R. Cao, L. Zhuo, J. Ren, J. Sun, J. Luo and X. Sun, *Nat. Commun.*, 2021, **12**, 238.
50 H. Sun, L. Chen, L. Xiong, K. Feng, Y. Chen, X. Zhang, X. Yuan, B. Yang, Z. Deng, Y. Liu, M. H. Rümmeli, J. Zhong, Y. Jiao and Y. Peng, *Nat. Commun.*, 2021, **12**, 6823.
51 C. Liu, X.-D. Zhang, J.-M. Huang, M.-X. Guan, M. Xu and Z.-Y. Gu, *ACS Catal.*, 2022, **12**, 15230–15240.
52 J. Du, B. Cheng, L. Jiang and Z. Han, *Chem. Commun.*, 2023, **59**, 4778–4781.
53 C. F. Wen, M. Zhou, X. Wu, Y. Liu, F. Mao, H. Q. Fu, Y. Shi, S. Dai, M. Zhu, S. Yang, H. F. Wang, P. F. Liu and H. G. Yang, *J. Mater. Chem. A*, 2023, **11**, 12121–12129.
54 H. Zhang, C. Zhu, R. Liu, Q. Fang, S. Song and Y. Shen, *Appl. Catal., B*, 2024, **343**, 123566.
55 L. Fan, Q. Geng, L. Ma, C. Wang, J.-X. Li, W. Zhu, R. Shao, W. Li, X. Feng, Y. Yamauchi, C. Li and L. Jiang, *Chem. Sci.*, 2023, **14**, 13851–13859.
56 Y. Huo, X. Peng, X. Liu, H. Li and J. Luo, *ACS Appl. Mater. Interfaces*, 2018, **10**, 12618–12625.
57 Y. Shen, Y. Pan, H. Xiao, H. Zhang, C. Zhu, Q. Fang, Y. Li, L. Lu, L. Ye and S. Song, *J. Mater. Chem. A*, 2024, **12**, 9075–9087.
58 C. F. Wen, M. Zhou, P. F. Liu, Y. Liu, X. Wu, F. Mao, S. Dai, B. Xu, X. L. Wang, Z. Jiang, P. Hu, S. Yang, H. F. Wang and H. G. Yang, *Angew. Chem., Int. Ed.*, 2022, **61**, e202111700.
59 P.-P. Guo, Z.-H. He, S.-Y. Yang, W. Wang, K. Wang, C.-C. Li, Y.-Y. Wei, Z.-T. Liu and B. Han, *Green Chem.*, 2022, **24**, 1527–1533.
60 Z. Yang, X. Wen, X. Guo, Y. Chen, L. Gao, R. Wei, X. Pan, J. Zhang and G. Xiao, *Sep. Purif. Technol.*, 2024, **332**, 125870.

Open Access Article. Published on 27 2025. Downloaded on 14-02-2026 07:37:44.
This article is licensed under a Creative Commons Attribution 3.0 Unported Licence.

61 A. Stalinraja, K. Gopalram, S. Venkatesan, M. J. Swamynathan, S. Ghosh and T. Selvaraj, *Electrochim. Acta*, 2022, **431**, 141078.
62 Z. Yang, X. Wen, X. Guo, Y. Chen, R. Wei, L. Gao, X. Pan, J. Zhang and G. Xiao, *J. Colloid Interface Sci.*, 2023, **650**, 1446–1456.
63 X. Yuan, S. Chen, D. Cheng, L. Li, W. Zhu, D. Zhong, Z. J. Zhao, J. Li, T. Wang and J. Gong, *Angew. Chem., Int. Ed.*, 2021, **133**, 15472–15475.
64 T. Zhao, J. Li, J. Liu, F. Liu, K. Xu, M. Yu, W. Xu and F. Cheng, *ACS Catal.*, 2023, **13**, 4444–4453.
65 S. Hong, H. G. Abbas, K. Jang, K. K. Patra, B. Kim, B.-U. Choi, H. Song, K.-S. Lee, P.-P. Choi, S. Ringe and J. Oh, *Adv. Mater.*, 2023, **35**, 2208996.
66 Y. Zhang, H. Zhang, S. Xie, Z. Hou, T. Xu, Y. Shang and Z. Yan, *New J. Chem.*, 2022, **46**, 17244–17250.
67 S. Chu, X. Yan, C. Choi, S. Hong, A. W. Robertson, J. Masa, B. Han, Y. Jung and Z. Sun, *Green Chem.*, 2020, **22**, 6540–6546.
68 Z.-Y. Zhang, H. Tian, H. Jiao, X. Wang, L. Bian, Y. Liu, N. Khaorapapong, Y. Yamauchi and Z.-L. Wang, *J. Mater. Chem. A*, 2024, **12**, 1218–1232.
69 S. Sultan, H. Lee, S. Park, M. M. Kim, A. Yoon, H. Choi, T.-H. Kong, Y.-J. Ko, H.-S. Oh, Z. Lee, H. Kim, W. Kim and Y. Kwon, *Energy Environ. Sci.*, 2022, **15**, 2397–2409.
70 X. Wang, Y. Jiang, K. Mao, W. Gong, D. Duan, J. Ma, Y. Zhong, J. Li, H. Liu, R. Long and Y. Xiong, *J. Am. Chem. Soc.*, 2022, **144**, 22759–22766.
71 S. Kwon, J. Zhang, R. Ganganahalli, S. Verma and B. S. Yeo, *Angew. Chem., Int. Ed.*, 2023, **62**, e202217252.
72 Y. Zhou and B. S. Yeo, *J. Mater. Chem. A*, 2020, **8**, 23162–23186.
73 M. Li, F. Zhang, M. Kuang, Y. Ma, T. Liao, Z. Sun, W. Luo, W. Jiang and J. Yang, *Nano-Micro Lett.*, 2023, **15**, 238.
74 S. Yi, Z. Wang, Z. Wu, X. Yang, H. Wang, J. Yang, X. She and H. Xu, *Appl. Surf. Sci.*, 2025, **681**, 161492.
75 C. Chen, X. Yan, S. Liu, Y. Wu, Q. Wan, X. Sun, Q. Zhu, H. Liu, J. Ma, L. Zheng, H. Wu and B. Han, *Angew. Chem., Int. Ed.*, 2020, **132**, 16601–16606.
76 L. Huang, Z. Liu, G. Gao, C. Chen, Y. Xue, J. Zhao, Q. Lei, M. Jin, C. Zhu, Y. Han, J. S. Francisco and X. Lu, *J. Am. Chem. Soc.*, 2023, **145**, 26444–26451.
77 K. Hara, N. Sonoyama and T. Sakata, *Bull. Chem. Soc. Jpn.*, 2006, **70**, 745–754.
78 G. Centi, S. Perathoner, G. Winè and M. Gangeri, *Green Chem.*, 2007, **9**, 671–678.
79 R. Shiratsuchi and G. Nogami, *J. Electrochem. Soc.*, 1996, **143**, 582.
80 W. Zhang, J. Ai, T. Ouyang, L. Yu, A. Liu, L. Han, Y. Duan, C. Tian, C. Chu, Y. Ma, S. Che and Y. Fang, *J. Am. Chem. Soc.*, 2024, **146**, 28214–28221.
81 H. Yoshio, M. Akira, T. Ryutaro and S. Shin, *Chem. Lett.*, 1987, 1665–1668.
82 R. L. Cook, R. C. MacDuff and A. F. Sammells, *J. Electrochem. Soc.*, 1990, **137**, 187.
83 Y. Hori, H. Wakebe, T. Tsukamoto and O. Koga, *Electrochim. Acta*, 1994, **39**, 1833–1839.
84 T. Saeki, K. Hashimoto, N. Kimura, K. Omata and A. Fujishima, *J. Electroanal. Chem.*, 1996, **404**, 299–302.
85 S. Nellaiappan and S. Sharma, *ACS Appl. Energy Mater.*, 2019, **2**, 2998–3003.
86 Y. Zhou, A. J. Martín, F. Dattila, S. Xi, N. López, J. Pérez-Ramírez and B. S. Yeo, *Nat. Catal.*, 2022, **5**, 545–554.
87 R. E. Vos and M. T. M. Koper, *ACS Catal.*, 2024, **14**, 4432–4440.
88 Y. Xiao, J. Lu, K. Chen, Y. Cao, C. Gong and F.-S. Ke, *Angew. Chem., Int. Ed.*, 2024, **63**, e202404738.
89 X. Suo, F. Zhang, Z. Yang, L. Wang, M. Lei, J. A. Gaugler, M. Li, J. Fan, B. P. Thapaliya, I. Popovs, A. S. Ivanov, L. C. Gallington, D.-E. Jiang, Z. Liu and S. Dai, *Chem Catal.*, 2023, **3**, 100506.
90 B. Cao, F.-Z. Li, S. Han, Q. Xu and J. Gu, *ChemElectroChem*, 2025, **12**, e202400595.
91 Y. Zhang, Q. Zhou, X.-Y. Lu, X.-Y. Zhang, F. Gong and W.-Y. Sun, *CCS Chem.*, 2024, **6**, 2950–2960.
92 Z. Yang, X. Guo, Y. Chen, L. Gao, R. Wei, X. Pan and G. Xiao, *Chem. Eng. J.*, 2024, **495**, 153506.
93 C. Liang, B. Kim, S. Yang, L. Yang, C. Francisco Woellner, Z. Li, R. Vajtai, W. Yang, J. Wu, P. J. A. Kenis and P. M. Ajayan, *J. Mater. Chem. A*, 2018, **6**, 10313–10319.
94 S. Singh, R. K. Gautam, K. Malik and A. Verma, *J. CO2 Util.*, 2017, **18**, 139–146.
95 X. Wang, Z. Jiang, P. Wang, Z. Chen, T. Sheng, Z. Wu and Y. Xiong, *Angew. Chem., Int. Ed.*, 2023, **62**, e202313646.
96 R. Kortlever, I. Peters, C. Balemans, R. Kas, Y. Kwon, G. Mul and M. T. M. Koper, *Chem. Commun.*, 2016, **52**, 10229–10232.
97 S. Y. Hwang, J. Y. Maeng, G. E. Park, S. Y. Yang, S. Y. Kim, C. K. Rhee and Y. Sohn, *Chemosphere*, 2023, **338**, 139616.
98 Y. J. Kim, J. Y. Maeng, S. Y. Hwang, C. K. Rhee and Y. Sohn, *Appl. Catal., B*, 2023, **338**, 123017.
99 Y. J. Kim, J. Y. Maeng, S. Y. Hwang, J. H. Yang, I. Yoon, C. W. Myung, C. K. Rhee and Y. Sohn, *Nano Energy*, 2023, **118**, 108995.
100 S. Y. Kim, S. Y. Hwang, J. Y. Maeng, C. K. Rhee and Y. Sohn, *Int. J. Hydrogen Energy*, 2024, **51**, 571–587.
101 D. van den Berg, B. Izelaar, S. Fu and R. Kortlever, *Catal. Sci. Technol.*, 2024, **14**, 555–561.
102 D. A. Torelli, S. A. Francis, J. C. Crompton, A. Javier, J. R. Thompson, B. S. Brunschwig, M. P. Soriaga and N. S. Lewis, *ACS Catal.*, 2016, **6**, 2100–2104.
103 A. R. Paris and A. B. Bocarsly, *ACS Catal.*, 2017, **7**, 6815–6820.
104 J. Y. Maeng, S. Y. Hwang, C. K. Rhee and Y. Sohn, *Appl. Surf. Sci.*, 2023, **631**, 157576.
105 Y. Ji, X. Lv, R. Wei, A. Guan, C. Yang, Y. Yan, M. Kuang and G. Zheng, *Angew. Chem., Int. Ed.*, 2024, **63**, e202411194.
106 T. V. Magdesieva, T. Yamamoto, D. A. Tryk and A. Fujishima, *J. Electrochem. Soc.*, 2002, **149**, D89.
107 J. Du, B. Cheng, H. Yuan, Y. Tao, Y. Chen, M. Ming, Z. Han and R. Eisenberg, *Angew. Chem., Int. Ed.*, 2023, **62**, e202211804.
108 F. Guo, R.-X. Li, S. Yang, X.-Y. Zhang, H. Yu, J. J. Urban and W.-Y. Sun, *Angew. Chem., Int. Ed.*, 2023, **62**, e202216232.
109 C. C. Lee, Y. Hu and M. W. Ribbe, *Angew. Chem., Int. Ed.*, 2015, **127**, 1235–1238.
110 K. Tanifuji, N. Sickerman, C. C. Lee, T. Nagasawa, K. Miyazaki, Y. Ohki, K. Tatsumi, Y. Hu and M. W. Ribbe, *Angew. Chem., Int. Ed.*, 2016, **128**, 15862–15865.

© 2025 The Author(s). Published by the Royal Society of Chemistry

Open Access Article. Published on 27 2025. Downloaded on 14-02-2026 07:37:44.
This article is licensed under a Creative Commons Attribution 3.0 Unported Licence.

111 N. S. Sickerman, K. Tanifuji, C. C. Lee, Y. Ohki, K. Tatsumi, M. W. Ribbe and Y. Hu, *J. Am. Chem. Soc.*, 2017, **139**, 603–606.
112 J. Wu, S. Ma, J. Sun, J. I. Gold, C. Tiwary, B. Kim, L. Zhu, N. Chopra, I. N. Odeh, R. Vajtai, A. Z. Yu, R. Luo, J. Lou, G. Ding, P. J. A. Kenis and P. M. Ajayan, *Nat. Commun.*, 2016, **7**, 13869.
113 X. Zou, M. Liu, J. Wu, P. M. Ajayan, J. Li, B. Liu and B. I. Yakobson, *ACS Catal.*, 2017, **7**, 6245–6250.
114 R. Feng, Q. Zhu, M. Chu, S. Jia, J. Zhai, H. Wu, P. Wu and B. Han, *Green Chem.*, 2020, **22**, 7560–7565.
115 T. Zhang, W. Li, K. Huang, H. Guo, Z. Li, Y. Fang, R. M. Yadav, V. Shanov, P. M. Ajayan, L. Wang, C. Lian and J. Wu, *Nat. Commun.*, 2021, **12**, 5265.
116 R. M. Yadav, Z. Li, T. Zhang, O. Sahin, S. Roy, G. Gao, H. Guo, R. Vajtai, L. Wang, P. M. Ajayan and J. Wu, *Adv. Mater.*, 2022, **34**, 2105690.
117 A. F. Pérez-Cadenas, C. H. Ros, S. Morales-Torres, M. Pérez-Cadenas, P. J. Kooyman, C. Moreno-Castilla and F. Kapteijn, *Carbon*, 2013, **56**, 324–331.
118 A. Abdelwahab, J. Castelo-Quibén, M. Pérez-Cadenas, A. Elmouwahidi, F. J. Maldonado-Hódar, F. Carrasco-Marín and A. F. Pérez-Cadenas, *Catalysts*, 2017, **7**, 25.
119 W. Cai, J. Yin, C. Hu, H. Han, J. Ma, Y. Cao and Y. Zhao, *Catal. Lett.*, 2022, **153**, 2718–2727.
120 Y. Cui, C. Yang, H. Lin, S. Rui, D. Yao, Y. Liao, C. Zhang, Y. Fang, X. Wang, Z. Zhong, Y. Song, G. Wang, L. Zhuang and Z. Li, *ACS Catal.*, 2023, **13**, 169–178.
121 B. M. Pirzada, F. AlMarzooqi and A. Qurashi, *Ultrason. Sonochem.*, 2025, **112**, 107189.
122 J. Liu, P. Li, J. Bi, S. Jia, Y. Wang, X. Kang, X. Sun, Q. Zhu and B. Han, *J. Am. Chem. Soc.*, 2023, **145**, 23037–23047.
123 Y. Jiang, C. Choi, S. Hong, S. Chu, T.-S. Wu, Y.-L. Soo, L. Hao, Y. Jung and Z. Sun, *Cell Rep. Phys. Sci.*, 2021, **2**, 100356.
124 J. Wan, L. Lin, T. Yang and Y. Li, *Electrochim. Acta*, 2022, **421**, 140488.
125 Q. Wan, J. Zhang, B. Zhang, D. Tan, L. Yao, L. Zheng, F. Zhang, L. Liu, X. Cheng and B. Han, *Green Chem.*, 2020, **22**, 2750–2754.
126 R. Du, Q. Wu, S. Zhang, P. Wang, Z. Li, Y. Qiu, K. Yan, G. I. N. Waterhouse, P. Wang, J. Li, Y. Zhao, W.-W. Zhao, X. Wang and G. Chen, *Small*, 2023, **19**, 2301289.
127 I. Merino-Garcia, J. Albo, J. Solla-Gullón, V. Montiel and A. Irabien, *J. CO2 Util.*, 2019, **31**, 135–142.
128 Y. Yan, Z. Zhao, J. Zhao, Y. Xu, Y. Xu, Y. Zhao, W. Tang and J.-M. Lee, *ACS Mater. Lett.*, 2021, **3**, 1143–1150.
129 Y. Yan, Z. Zhao, J. Zhao, W. Tang, W. Huang and J.-M. Lee, *J. Mater. Chem. A*, 2021, **9**, 7496–7502.
130 B. Chen, L. Gong, N. Li, H. Pan, Y. Liu, K. Wang and J. Jiang, *Adv. Funct. Mater.*, 2024, **34**, 2310029.
131 Q. Mo, S. Li, C. Chen, H. Song, Q. Gao and L. Zhang, *ACS Sustainable Chem. Eng.*, 2024, **12**, 6093–6101.
132 Q. Li, J. Wu, L. Lv, L. Zheng, Q. Zheng, S. Li, C. Yang, C. Long, S. Chen and Z. Tang, *Adv. Mater.*, 2024, **36**, 2305508.
133 D. Tan, B. Wulan, X. Cao and J. Zhang, *Nano Energy*, 2021, **89**, 106460.
134 L. Xiong, X. Zhang, H. Yuan, J. Wang, X. Yuan, Y. Lian, H. Jin, H. Sun, Z. Deng, D. Wang, J. Hu, H. Hu, J. Choi, J. Li, Y. Chen, J. Zhong, J. Guo, M. H. Rümmerli, L. Xu and Y. Peng, *Angew. Chem., Int. Ed.*, 2021, **60**, 2508–2518.
135 D. Wang, Q. Song, K. Li, Y. Zhou, J. Mao, C. Zhang, Y. Lou, C. Pan, J. Zhang, Y. Zhu and Y. Zhang, *J. Mater. Chem. A*, 2024, **12**, 11968–11974.
136 J. Y. Kim, Y. Kim, C. H. Ryu and H. S. Ahn, *Green Chem.*, 2023, **25**, 5290–5295.
137 D. Shu, M. Wang, F. Tian, H. Zhang and C. Peng, *J. CO2 Util.*, 2021, **45**, 101444.
138 M. Liu, Q. Wang, T. Luo, M. Herran, X. Cao, W. Liao, L. Zhu, H. Li, A. Stefancu, Y.-R. Lu, T.-S. Chan, E. Pensa, C. Ma, S. Zhang, R. Xiao and E. Cortés, *J. Am. Chem. Soc.*, 2024, **146**, 468–475.
139 F.-Y. Gao, R.-C. Bao, M.-R. Gao and S.-H. Yu, *J. Mater. Chem. A*, 2020, **8**, 15458–15478.
140 Y. Cui, Y. Cheng, C. Yang, Y. Su, D. Yao, B. Liufu, J. Li, Y. Fang, S. Liu, Z. Zhong, X. Wang, Y. Song and Z. Li, *ACS Sustainable Chem. Eng.*, 2023, **11**, 11229–11238.
141 M. Z. Iqbal, S. Imteyaz, C. Ghanty and S. Sarkar, *J. Ind. Eng. Chem.*, 2022, **113**, 15–31.
142 J. Rosen, G. S. Hutchings, Q. Lu, R. V. Forest, A. Moore and F. Jiao, *ACS Catal.*, 2015, **5**, 4586–4591.
143 J. Chen, D. Wang, X. Yang, W. Cui, X. Sang, Z. Zhao, L. Wang, Z. Li, B. Yang, L. Lei, J. Zheng, L. Dai and Y. Hou, *Angew. Chem., Int. Ed.*, 2023, **62**, e202215406.
144 J. C. Weiss, Y. He, D. A. Cullen, A. Benavidez, J. D. Jernigen, H. Zhang, L. Osmieri and P. Zelenay, *Small*, 2025, **21**, 2412162.
145 Z. Han, R. Kortlever, H.-Y. Chen, J. C. Peters and T. Agapie, *ACS Cent. Sci.*, 2017, **3**, 853–859.
146 D.-H. Nam, P. De Luna, A. Rosas-Hernández, A. Thevenon, F. Li, T. Agapie, J. C. Peters, O. Shekhah, M. Eddaoudi and E. H. Sargent, *Nat. Mater.*, 2020, **19**, 266–276.
147 T. Akter, H. Pan and C. J. Barile, *J. Phys. Chem. C*, 2022, **126**, 10045–10052.
148 T. Akter and C. J. Barile, *J. Mater. Chem. A*, 2023, **11**, 11354–11363.
149 H. Pan, T. Akter and C. J. Barile, *ACS Appl. Energy Mater.*, 2022, **5**, 12860–12868.
150 S. Han, W. Xia, S. Jia, T. Yao, J. Jiao, M. Wang, X. Dong, J. Yang, D. Zhou, M. He, H. Wu and B. Han, *ChemCatChem*, 2024, **16**, e202300918.
151 D. Song, Y. Lian, M. Wang, Y. Su, F. Lyu, Z. Deng and Y. Peng, *eScience*, 2023, **3**, 100097.
152 M. Li, S. Kuang, H. Liu, Q. Fan, S. Zhang and X. Ma, *J. Phys. Chem. C*, 2023, **127**, 3952–3959.
153 L. Xue, Z. Gao, T. Ning, W. Li, J. Li, J. Yin, L. Xiao, G. Wang and L. Zhuang, *Angew. Chem., Int. Ed.*, 2023, **62**, e202309519.
154 J. C. Bui, C. Kim, A. J. King, O. Romiluyi, A. Kusoglu, A. Z. Weber and A. T. Bell, *Acc. Chem. Res.*, 2022, **55**, 484–494.
155 O. Christensen, S. Zhao, Z. Sun, A. Bagger, J. V. Lauritsen, S. U. Pedersen, K. Daasbjerg and J. Rossmeisl, *ACS Catal.*, 2022, **12**, 15737–15749.

Open Access Article. Published on 27 2025. Downloaded on 14-02-2026 07:37:44.
This article is licensed under a Creative Commons Attribution 3.0 Unported Licence.

156 M. Jun, D. Kim, M. Kim, M. Kim, T. Kwon and K. Lee, *ACS Omega*, 2022, **7**, 42655–42663.
157 D. Xiao, X. Bao, M. Zhang, Z. Li, Z. Wang, Y. Gao, Z. Zheng, P. Wang, H. Cheng, Y. Liu, Y. Dai and B. Huang, *Chem. Eng. J.*, 2023, **452**, 139358.
158 S. Min, Z. Wang, X. Xu, J. He, M. Sun, W. Lin and L. Kang, *Appl. Surf. Sci.*, 2024, **663**, 160150.
159 M. Ma, L. Xiong, Y. Dong, Q. Bai, W. Hua, Z. Zheng, F. Lyu, Y. Lian, Z. Wei, H. Yuan, Z. Jiao, J. Cheng, D. Song, M. Wang, Z. Xing, J. Zhong, S. Han, Z. Deng and Y. Peng, *Adv. Funct. Mater.*, 2024, **34**, 2315667.
160 W. Li, L. Li, Q. Xia, S. Hong, L. Wang, Z. Yao, T.-S. Wu, Y.-L. Soo, H. Zhang, T. W. B. Lo, A. W. Robertson, Q. Liu, L. Hao and Z. Sun, *Appl. Catal., B*, 2022, **318**, 121823.
161 J. Feng, L. Wu, S. Liu, L. Xu, X. Song, L. Zhang, Q. Zhu, X. Kang, X. Sun and B. Han, *J. Am. Chem. Soc.*, 2023, **145**, 9857–9866.
162 X. Yan, C. Chen, Y. Wu, S. Liu, Y. Chen, R. Feng, J. Zhang and B. Han, *Chem. Sci.*, 2021, **12**, 6638–6645.
163 R. P. Singh, P. Arora, S. Nellaiappan, C. Shivakumara, S. Irusta, M. Paliwal and S. Sharma, *Electrochim. Acta*, 2019, **326**, 134952.
164 R. M. Arán-Ais, F. Scholten, S. Kunze, R. Rizo and B. Roldan Cuenya, *Nat. Energy*, 2020, **5**, 317–325.
165 X. He, L. Lin, X. Li, M. Zhu, Q. Zhang, S. Xie, B. Mei, F. Sun, Z. Jiang, J. Cheng and Y. Wang, *Nat. Commun.*, 2024, **15**, 9923.
166 B. Roldán Cuenya, F. Scholten, K.-L. C. Nguyen, J. P. Bruce and M. Heyde, *Angew. Chem., Int. Ed.*, 2021, **60**, 19169–19175.
167 Y. Zhang, P. Li, C. Zhao, G. Zhou, F. Zhou, Q. Zhang, C. Su and Y. Wu, *Sci. Bull.*, 2022, **67**, 1679–1687.
168 Y. Zheng, J. Zhang, Z. Ma, G. Zhang, H. Zhang, X. Fu, Y. Ma, F. Liu, M. Liu and H. Huang, *Small*, 2022, **18**, 2201695.
169 X. Mao, C.-W. Chang, Z. Li, Z. Han, J. Gao, M. Lyons, G. Sterbinsky, Y. Guo, B. Zhang, Y. Wang, X. Wang, D. Han, Q.-H. Yang, Z. Feng and Z. Weng, *Adv. Energy Mater.*, 2024, **14**, 2400827.
170 S. Wang, H. Chen, W. Lin, W. Zhou, X. Lv, J. Wang and J. Fu, *Ind. Eng. Chem. Res.*, 2022, **61**, 16445–16452.
171 J. Feng, W. Zhang, D. Shi, Y. Jia, Y. Tang, Y. Meng and Q. Gao, *Chem. Sci.*, 2024, **15**, 9173–9182.
172 X. Wu, Z. Tong, Y. Liu, Y. Li, Y. Cheng, J. Yu, P. Cao, C. Zhuang, Q. Shi, N. Liu, X. Liu, H. Liang and H. Li, *Nano Res.*, 2024, **17**, 7194–7202.
173 D. Kim, H. Yun, J. Kim, C. W. Lee and Y. J. Hwang, *J. Mater. Chem. A*, 2024, **12**, 23780–23788.
174 Y. Ji, Z. Chen, R. Wei, C. Yang, Y. Wang, J. Xu, H. Zhang, A. Guan, J. Chen, T.-K. Sham, J. Luo, Y. Yang, X. Xu and G. Zheng, *Nat. Catal.*, 2022, **5**, 251–258.
175 J. Huang, J. Dai, J. Zhu, R. Chen, X. Fu, H. Liu and G. Li, *J. Catal.*, 2022, **415**, 134–141.
176 J. Zhang, C. Guo, S. Fang, X. Zhao, L. Li, H. Jiang, Z. Liu, Z. Fan, W. Xu, J. Xiao and M. Zhong, *Nat. Commun.*, 2023, **14**, 1298.
177 X. Chen, D. A. Henckel, U. O. Nwabara, Y. Li, A. I. Frenkel, T. T. Fister, P. J. A. Kenis and A. A. Gewirth, *ACS Catal.*, 2020, **10**, 672–682.
178 D. Zhou, C. Chen, Y. Zhang, M. Wang, S. Han, X. Dong, T. Yao, S. Jia, M. He, H. Wu and B. Han, *Angew. Chem., Int. Ed.*, 2024, **63**, e202400439.
179 Y. Zhou, F. Che, M. Liu, C. Zou, Z. Liang, P. De Luna, H. Yuan, J. Li, Z. Wang, H. Xie, H. Li, P. Chen, E. Bladt, R. Quintero-Bermudez, T.-K. Sham, S. Bals, J. Hofkens, D. Sinton, G. Chen and E. H. Sargent, *Nat. Chem.*, 2018, **10**, 974–980.
180 M. Azuma, K. Hashimoto, M. Hiramoto, M. Watanabe and T. Sakata, *J. Electroanal. Chem. Interfacial Electrochem.*, 1989, **260**, 441–445.
181 K. U. D. Calvinho, A. B. Laursen, K. M. K. Yap, T. A. Goetjen, S. Hwang, N. Murali, B. Mejia-Sosa, A. Lubarski, K. M. Teeluck, E. S. Hall, E. Garfunkel, M. Greenblatt and G. C. Dismukes, *Energy Environ. Sci.*, 2018, **11**, 2550–2559.
182 X.-H. Liu, X.-L. Jia, Y.-L. Zhao, R.-X. Zheng, Q.-L. Meng, C.-P. Liu, W. Xing and M.-L. Xiao, *Adv. Sen. Energy Mater.*, 2023, **2**, 100073.
183 A. Mustafa, Y. Shuai, B. G. Lougou, Z. Wang, S. Razzaq, J. Zhao and J. Shan, *Chem. Eng. Sci.*, 2021, **245**, 116869.
184 R. Kortlever, C. Balemans, Y. Kwon and M. T. M. Koper, *Catal. Today*, 2015, **244**, 58–62.
185 X. Bai, W. Chen, C. Zhao, S. Li, Y. Song, R. Ge, W. Wei and Y. Sun, *Angew. Chem., Int. Ed.*, 2017, **129**, 12387–12391.
186 H. Huang, H. Jia, Z. Liu, P. Gao, J. Zhao, Z. Luo, J. Yang and J. Zeng, *Angew. Chem., Int. Ed.*, 2017, **56**, 3594–3598.
187 L. Lu, X. Sun, J. Ma, D. Yang, H. Wu, B. Zhang, J. Zhang and B. Han, *Angew. Chem., Int. Ed.*, 2018, **57**, 14149–14153.
188 M. Rahaman, K. Kiran, I. Z. Montiel, V. Grozovski, A. Dutta and P. Broekmann, *Green Chem.*, 2020, **22**, 6497–6509.
189 M. Usman, M. Humayun, M. D. Garba, L. Ullah, Z. Zeb, A. Helal, M. H. Suliman, B. Y. Alfaifi, N. Iqbal, M. Abdinejad, A. A. Tahir and H. Ullah, *Nanomaterials*, 2021, **11**, 2029.
190 M. Wang, K. Torbensen, D. Salvatore, S. Ren, D. Joulié, F. Dumoulin, D. Mendoza, B. Lassalle-Kaiser, U. Işci, C. P. Berlinguette and M. Robert, *Nat. Commun.*, 2019, **10**, 3602.
191 S. Gao, Y. Lin, X. Jiao, Y. Sun, Q. Luo, W. Zhang, D. Li, J. Yang and Y. Xie, *Nature*, 2016, **529**, 68–71.
192 Q. Li, Y. Hou, J. Yin and P. Xi, *Catalysts*, 2023, **13**, 1384.
193 J. Du, S. Li, S. Liu, Y. Xin, B. Chen, H. Liu and B. Han, *Chem. Sci.*, 2020, **11**, 5098–5104.
194 Y. Hori, *Modern Aspects of Electrochemistry*, Springer, New York, 2008, vol. 42, pp. 89–189.
195 H. Wu, L. Huang, J. Timoshenko, K. Qi, W. Wang, J. Liu, Y. Zhang, S. Yang, E. Petit, V. Flaud, J. Li, C. Salameh, P. Miele, L. Lajaunie, B. Roldán Cuenya, D. Rao and D. Voiry, *Nat. Energy*, 2024, **9**, 422–433.
196 A. Marcos-Madrazo, C. Casado-Coterillo, J. Iniesta and A. Irabien, *Membranes*, 2022, **12**, 783.
197 J. Han, B. Tu, P. An, J. Zhang, Z. Yan, X. Zhang, C. Long, Y. Zhu, Y. Yuan, X. Qiu, Z. Yang, X. Huang, S. Yan and Z. Tang, *Adv. Mater.*, 2024, **36**, 2313926.
198 S. S. Lavate and R. Srivastava, *Energy Adv.*, 2024, **3**, 2801–2811.
199 Y. Wang, J. Wang, R. Cai, J. Zhang, S. Xia, Z. Li, C. Yu, J. Wu, P. Wang and Y. Wu, *Adv. Funct. Mater.*, 2024, 2417764.

© 2025 The Author(s). Published by the Royal Society of Chemistry

Open Access Article. Published on 27 2025. Downloaded on 14-02-2026 07:37:44. This article is licensed under a Creative Commons Attribution 3.0 Unported Licence.

200 M. Zhong, K. Tran, Y. Min, C. Wang, Z. Wang, C.-T. Dinh, P. De Luna, Z. Yu, A. S. Rasouli, P. Brodersen, S. Sun, O. Voznyy, C.-S. Tan, M. Askerka, F. Che, M. Liu, A. Seifitokaldani, Y. Pang, S.-C. Lo, A. Ip, Z. Ulissi and E. H. Sargent, *Nature*, 2020, **581**, 178–183.
201 Y. Yao, T. Shi, W. Chen, J. Wu, Y. Fan, Y. Liu, L. Cao and Z. Chen, *Nat. Commun.*, 2024, **15**, 1257.
202 Y. Sha, J. Zhang, X. Cheng, M. Xu, Z. Su, Y. Wang, J. Hu, B. Han and L. Zheng, *Angew. Chem., Int. Ed.*, 2022, **61**, e202200039.
203 Z.-Y. Zhang, H.-B. Wang, F.-F. Zhang, J.-W. Li, X.-Z. Hu, S.-W. Yan, Y.-M. Bai, X. Zhang, G.-R. Shen, P.-F. Yin, J. Yang, C.-K. Dong, J. Mao, H. Liu and X.-W. Du, *Rare Met.*, 2024, **43**, 1513–1523.
204 W. Zhou, H. Zheng, X. Li, N. Meng, C. Feng, H. Yang, Q. Hu and C. He, *Adv. Funct. Mater.*, 2024, **34**, 2311226.
205 H. Luo, B. Li, J.-G. Ma and P. Cheng, *Angew. Chem., Int. Ed.*, 2022, **61**, e202116736.
206 H. Tao, F. Wang, Z. Zhang and S. Min, *Sustainable Energy Fuels*, 2023, **7**, 2991–2996.
207 B. Cheng, J. Du, H. Yuan, Y. Tao, Y. Chen, J. Lei and Z. Han, *ACS Appl. Mater. Interfaces*, 2022, **14**, 27823–27832.
208 W. Xue, H. Liu, X. Chen, X. Yang, R. Yang, Y. Liu, M. Li, X. Yang, B. Y. Xia and B. You, *Sci. China Chem.*, 2023, **66**, 1834–1843.
209 G. Dong, G. Wang, J. Cheng, M. Li, Z. Liang, D. Geng and W. Tang, *Appl. Catal., B*, 2024, **342**, 123444.
210 Y. Wang, X. Wei, Y. Li, J. Luo, L. Chen and J. Shi, *Chem. Eng. J.*, 2024, **485**, 149800.
211 F. Li, A. Thevenon, A. Rosas-Hernández, Z. Wang, Y. Li, C. M. Gabardo, A. Ozden, C. T. Dinh, J. Li, Y. Wang, J. P. Edwards, Y. Xu, C. McCallum, L. Tao, Z.-Q. Liang, M. Luo, X. Wang, H. Li, C. P. O'Brien, C.-S. Tan, D.-H. Nam, R. Quintero-Bermudez, T.-T. Zhuang, Y. C. Li, Z. Han, R. D. Britt, D. Sinton, T. Agapie, J. C. Peters and E. H. Sargent, *Nature*, 2020, **577**, 509–513.
212 L. Bian, Z.-Y. Zhang, H. Tian, N.-N. Tian, Z. Ma and Z.-L. Wang, *Chin. J. Catal.*, 2023, **54**, 199–211.
213 C. Zhang, Y. Gu, Q. Jiang, Z. Sheng, R. Feng, S. Wang, H. Zhang, Q. Xu, Z. Yuan and F. Song, *Nano-Micro Lett.*, 2024, **17**, 66.
214 J. Liu, K. Yu, Z. Qiao, Q. Zhu, H. Zhang and J. Jiang, *ChemSusChem*, 2023, **16**, e202300601.
215 Q. He, H. Li, Z. Hu, L. Lei, D. Wang and T.-T. Li, *Angew. Chem., Int. Ed.*, 2024, **63**, e202407090.
216 J.-Y. Kim, D. Hong, J.-C. Lee, H. G. Kim, S. Lee, S. Shin, B. Kim, H. Lee, M. Kim, J. Oh, G.-D. Lee, D.-H. Nam and Y.-C. Joo, *Nat. Commun.*, 2021, **12**, 3765.
217 A. Thevenon, A. Rosas-Hernández, J. C. Peters and T. Agapie, *Angew. Chem., Int. Ed.*, 2019, **131**, 17108–17114.
218 X. Y. Zhang, Z. X. Lou, J. Chen, Y. Liu, X. Wu, J. Y. Zhao, H. Y. Yuan, M. Zhu, S. Dai, H. F. Wang, C. Sun, P. F. Liu and H. G. Yang, *Nat. Commun.*, 2023, **14**, 7681.
219 H. Bai, T. Cheng, S. Li, Z. Zhou, H. Yang, J. Li, M. Xie, J. Ye, Y. Ji, Y. Li, Z. Zhou, S. Sun, B. Zhang and H. Peng, *Sci. Bull.*, 2021, **66**, 62–68.
220 W. Yang, H. Liu, Y. Qi, Y. Li, Y. Cui, L. Yu, X. Cui and D. Deng, *J. Energy Chem.*, 2023, **85**, 102–107.
221 J. Wang, W. Li, J. Peng, S. Shang, X. Fu, G. He and Q. Zhang, *Vacuum*, 2024, **222**, 113017.
222 Y. Wang, Z. Wang, C.-T. Dinh, J. Li, A. Ozden, M. Golam Kibria, A. Seifitokaldani, C.-S. Tan, C. M. Gabardo, M. Luo, H. Zhou, F. Li, Y. Lum, C. McCallum, Y. Xu, M. Liu, A. Proppe, A. Johnston, P. Todorovic, T.-T. Zhuang, D. Sinton, S. O. Kelley and E. H. Sargent, *Nat. Catal.*, 2019, **3**, 98–106.
223 Z. Wang, Y. Li, X. Zhao, S. Chen, Q. Nian, X. Luo, J. Fan, D. Ruan, B.-Q. Xiong and X. Ren, *J. Am. Chem. Soc.*, 2023, **145**, 6339–6348.
224 Y. Chae, K. Kim, H. Yun, D. Kim, W. Jung, Y. J. Hwang, U. Lee, D. K. Lee, B. K. Min, W. Choi and D. H. Won, *J. Mater. Chem. A*, 2023, **11**, 7025–7033.
225 Y. C. Tan, W. K. Quek, B. Kim, S. Sugiarto, J. Oh and D. Kai, *ACS Energy Lett.*, 2022, **7**, 2012–2023.
226 F. Bernasconi, A. Senocrate, P. Kraus and C. Battaglia, *EES Catal.*, 2023, **1**, 1009–1016.
227 S. T. Ahn, I. Abu-Baker and G. T. R. Palmore, *Catal. Today*, 2017, **288**, 24–29.
228 H. Yoshio, K. Katsuhei, M. Akira and S. Shin, *Chem. Lett.*, 1986, 897–898.
229 H. Song, J. T. Song, B. Kim, Y. C. Tan and J. Oh, *Appl. Catal., B*, 2020, **272**, 119049.
230 M. Moradzaman, C. S. Martínez and G. Mul, *Sustainable Energy Fuels*, 2020, **4**, 5195–5202.
231 M. Ma, W. Deng, A. Xu, D. Hochfilzer, Y. Qiao, K. Chan, I. Chorkendorff and B. Seger, *Energy Environ. Sci.*, 2022, **15**, 2470–2478.
232 B. Sahin, J. J. Leung, E. Magori, S. Laumen, A. Tawil, E. Simon and O. Hinrichsen, *Energy Technol.*, 2022, **10**, 2200972.
233 R. Kas, R. Kortlever, H. Yılmaz, M. T. M. Koper and G. Mul, *ChemElectroChem*, 2015, **2**, 354–358.
234 M. V. Khenkin, E. A. Katz, A. Abate, G. Bardizza, J. J. Berry, C. Brabec, F. Brunetti, V. Bulović, Q. Burlingame, A. Di Carlo, R. Cheacharoen, Y.-B. Cheng, A. Colsmann, S. Cros, K. Domanski, M. Dusza, C. J. Fell, S. R. Forrest, Y. Galagan, D. Di Girolamo, M. Grätzel, A. Hagfeldt, E. von Hauff, H. Hoppe, J. Kettle, H. Köbler, M. S. Leite, S. Liu, Y.-L. Loo, J. M. Luther, C.-Q. Ma, M. Madsen, M. Manceau, M. Matheron, M. McGehee, R. Meitzner, M. K. Nazeeruddin, A. F. Nogueira, Ç. Odabaşı, A. Osherov, N.-G. Park, M. O. Reese, F. De Rossi, M. Saliba, U. S. Schubert, H. J. Snaith, S. D. Stranks, W. Tress, P. A. Troshin, V. Turkovic, S. Veenstra, I. Visoly-Fisher, A. Walsh, T. Watson, H. Xie, R. Yıldırım, S. M. Zakeeruddin, K. Zhu and M. Lira-Cantu, *Nat. Energy*, 2020, **5**, 35–49.
235 E. Zimmermann, K. K. Wong, M. Müller, H. Hu, P. Ehrenreich, M. Kohlstädt, U. Würfel, S. Mastroianni, G. Mathiazhagan, A. Hinsch, T. P. Gujar, M. Thelakkat, T. Pfadler and L. Schmidt-Mende, *APL Mater.*, 2016, **4**, 091901–091907.
236 M. O. Reese, S. A. Gevorgyan, M. Jørgensen, E. Bundgaard, S. R. Kurtz, D. S. Ginley, D. C. Olson, M. T. Lloyd, P. Morvillo, E. A. Katz, A. Elschner, O. Haillant, T. R. Currier, V. Shrotriya, M. Hermenau, M. Riede, K. R. Kirov, G. Trimmel, T. Rath, O. Inganäs, F. Zhang, M. Andersson, K. Tvingstedt, M. Lira-Cantu, D. Laird, C. McGuiness, S. Gowrisanker,

Open Access Article. Published on 27 2025. Downloaded on 14-02-2026 07:37:44.
This article is licensed under a Creative Commons Attribution 3.0 Unported Licence.

M. Pannone, M. Xiao, J. Hauch, R. Steim, D. M. DeLongchamp, R. Rösch, H. Hoppe, N. Espinosa, A. Urbina, G. Yaman-Uzunoglu, J.-B. Bonekamp, A. J. J. M. van Breemen, C. Girotto, E. Voroshazi and F. C. Krebs, *Sol. Energy Mater. Sol. Cells*, 2011, **95**, 1253–1267.

237 B. Sahin, M. Kraehling, V. Facci Allegrini, J. Leung, K. Wiesner-Fleischer, E. Magori, R. Pastusiak, A. Tawil, T. Hodges, E. Brooke, E. C. Corbos, M. Fleischer, E. Simon and O. Hinrichsen, *J. CO2 Util.*, 2024, **82**, 102766.

238 Q. Xu, S. Garg, A. B. Moss, M. Mirolo, I. Chorkendorff, J. Drnec and B. Seger, *Nat. Catal.*, 2023, **6**, 1042–1051.

239 T. Zhang, Z. Li, X. Lyu, J. Raj, G. Zhang, H. Kim, X. Wang, S. Chae, L. Lemen, V. N. Shanov and J. Wu, *J. Electrochem. Soc.*, 2022, **169**, 104506.

240 J. M. Álvarez-Gómez and A. S. Varela, *Energy Fuels*, 2023, **37**, 15283–15308.

241 K. P. Kuhl, E. R. Cave, D. N. Abram and T. F. Jaramillo, *Energy Environ. Sci.*, 2012, **5**, 7050–7059.

242 X. Wang, C. Tomon, T. Bobrowski, P. Wilde, J. R. C. Junqueira, T. Quast, W. He, N. Sikdar, J. Weidner and W. Schuhmann, *ChemElectroChem*, 2022, **9**, e202200675.

243 Q. Chen, X. Luo, G. Mu, X. Mao, H. Yin, E. H. Lester and T. Wu, *ACS Sustainable Chem. Eng.*, 2024, **12**, 15134–15146.

244 Z. Wei, W. Wang, T. Shao, S. Yang, C. Liu, D. Si, R. Cao and M. Cao, *Angew. Chem., Int. Ed.*, 2025, **64**, e202417066.

245 Y. Zhou, R. Ganganahalli, S. Verma, H. R. Tan and B. S. Yeo, *Angew. Chem., Int. Ed.*, 2022, **61**, e202202859.

© 2025 The Author(s). Published by the Royal Society of Chemistry